Phytotaxa 470 (1): 001–030
https://www.mapress.com/j/pt/

Article

ISSN 1179-3155 (print edition)
PHYTOTAXA
ISSN 1179-3163 (online edition)

https://doi.org/10.11646/phytotaxa.470.1.1

Diatom genus *Planothidium* (Bacillariophyta) from streams and rivers in California, USA: diversity, distribution and autecology

ROSALINA STANCHEVA[1,3*], NATHANIEL V. KRISTAN[2,4], WILLIAM B. KRISTAN III[1,5] & ROBERT G. SHEATH[1,6]

[1] *Department of Biological Sciences, California State University San Marcos, San Marcos, California 92096, USA.*
[2] *Department of Oceanography, Humboldt State University, Arcata, California 95521, USA.*
[3] *rhristov@csusm.edu; https://orcid.org/0000-0003-0562-4026*
[4] *Nathaniel.Kristan@humboldt.edu; https://orcid.org/0000-0002-6058-0559*
[5] *wkristan@csusm.edu; https://orcid.org/0000-0001-7022-1034*
[6] *rsheath@csusm.edu*
**Corresponding author: rhistov@csusm.edu*

Abstract

The diatom genus *Planothidium* from streams and rivers in California was studied by applying the most current species designations. Twenty *Planothidium* taxa were identified in total, including a previously undescribed species, *Planothidium californicum*. Extensive light and scanning electron microscopic documentation is provided to support consistent further identification of the taxa for the local stream bioassessment. The most common and abundant species, recorded across the entire state, were *P. frequentissimum, P. lanceolatum*, *P. victorii, P. cryptolanceolatum*, *P. amphibium*, and *P. minutissimum*. Species ranges and species-weighted averages for the main anthropogenic stressors, i.e. chloride, conductivity, dissolved organic carbon, total nitrogen and total phosphorus were determined for the eleven most common *Planothdium* taxa. Statistically significant differences among species weighted averages were determined by randomization test. Of these eleven species, *P. delicatulum, P. robustum, P. engelbrechtii, P. frequentissimum* and *P. victorii* had the highest weighted averages along the chloride and conductivity gradients. *P. potapovae, Planothidium* sp. 1*, P. amphibium,* and *P. engelbrechtii* had narrow nutrient ranges and lowest weighted averages for total nitrogen and phosphorus, making them significantly different from *P. delicatulum* which had highest total nitrogen average and from *P. minutissimum*, associated with highest total phosphorus average level. Given that there were differences in associations with environmental variables between recently described species, it is important to use the new taxonomy when using diatoms in bioassessment work.

Keywords: *Planothidium*, Bacillariophyta, new species, streams, rivers, California, ecology, electron microscopy

Introduction

The members of the monoraphid diatom genus *Planothidium* Round & Bukhtiyarova are common and often abundant in streams with variable water quality (Morales 2006). *Planothidium* cells are usually solitary, with a convex rapheless valve (SV) and a slightly concave raphe valve (RV), adhered to the substratum, which could be aquatic plants, macroalgae (e.g., *Cladophora* Kützing*, Oedogonium* Link ex Hirn*, Vaucheria* A. P. de Candolle), colonial diatoms (eg. *Eunotia* Ehrenberg or *Pleurosira* (Meneghini) Trevisan), or inorganic sand grains (Round & Bukhtiyarova 1996a). *Planothidium* taxa have a great potential to serve as ecological indicators of stream condition and specific stressors such as eutrophication (Potapova & Charles 2007) or near-stream forest and wetland cover disturbance (Smucker *et al.* 2013). However, their challenging taxonomy (e. g., Lange-Bertalot & Krammer 1989, Krammer & Lange-Bertalot 1991, Morales 2006) and local species environmental associations need to be refined for a reliable bioassessment application.

The genus *Planothidium* was separated from *Achnanthes* Bory based on thick bi- to multiseriate striae interrupted on rapheless sternum valve (SV) unilaterally and marked by a "hoof-mark" depression (Round & Bukhtiyarova 1996b). The areolae number per stria and the shape of the SV depression (i.e. single or a double horse-shoe shaped mark, named a sinus or a cavum, respectively, Moss & Carter 1982), or a rimmed depression and a hood (Spaulding *et al.* 2008) are both important taxonomic features in delineating the species. Scanning electron microscopy (SEM)

Accepted by Evan Thomas: 11 Oct. 2020; published: 2 Nov. 2020

is needed for complete observation of these highly variable structures, because often their morphology is obscured under light microscope (LM). Furthermore, transitional forms complicate species identifications. Recently, several new freshwater *Planothidium* species have been published (i.e. Novis *et al.* 2012, Alvarez-Blanco & Blanco 2013, Blanco *et al.* 2013, Van de Vijver *et al.* 2013, 2018, Bąk & Lange-Bertalot 2014, Wetzel *et al.* 2014, 2019, Jahn *et al.* 2017), including from rivers in California (Stancheva 2019).

Freshwater algal bioassessment is based on ecological indicator value of morphologically identified taxa, using LM. The current trend in taxonomy is to use molecular identifications of algae in place of morphological identification (Zimmermann *et al.* 2014, Hering *et al.* 2018). However, gene sequence data for *P. lanceolatum* (Brébisson ex Kützing) Lange-Bertalot and *P. frequentissimum* (Lange-Bertalot) Lange-Bertalot species complexes are available from Europe and Asia only (Jahn *et al.* 2017).

For the last decade, the California Surface Water Ambient Monitoring Program (SWAMP) has used algae in stream bioassessment (Rehn 2016), but more recently has been collecting paired samples for both morphological and molecular algae identification from streams and rivers across the state. For the purpose of this study, we reanalyzed these diatom samples with LM and SEM, applying the new *Planothidium* species designations of Jahn *et al.* (2017), Van de Vijer *et al.* (2018), and Wetzel *et al.* (2013, 2019) aiming to: 1) refine *Planothidium* taxonomy and distribution; 2) determine statistically environmental ranges and optima for *Planothidium* species, and 3) provide morphological documentation of *Planothidium* taxa from samples, for which molecular data could be produced, for further comparison with *Planothidium* sequences from other continents (e.g., Jahn *et al.* 2017).

Material and methods

Sampling data set and diatom analysis

This study in based on 208 benthic algal samples, containing *Planothidium* taxa, collected from 183 wadeable streams across California as part of SWAMP projects in 2015 and 2016 as follows: perennial stream assessment, stormwater monitoring coalition assessment and non-perennial stream assessment in San Diego region (Supplemental Figure 7). The sampling locations for this study were selected to represent a wide range of environmental conditions across the state. Some sites were sampled both years. The diatom samples and environmental variables were collected quantitatively using the multihabitat sampling protocol (Fetscher *et al.* 2009). Chloride was measured as chloride anions by ion chromatography following EPA 300.0 protocol. At each stream reach, a composite algal sample with measured volume was collected using 11 random sampling points from the present substrata (e.g. cobble, silt/sand, gravel, bedrock, wood, etc.). The composite algal sample was then divided into 50 mL subsamples used for separate analysis of diatoms, non-diatom algae, and algal DNA extraction. The samples for DNA extraction were processed at the Southern California Coastal Water Research Project, Costa Mesa, California.

Additional diatom samples for this study were obtained from four non-wadeable rivers in California sampled in 2018 as part of the United States Environmental Protection Agency`s National Rivers and Streams Assessment Program (NRSA). Quantitative composite benthic diatom samples were collected from whatever substrata were present (e.g., cobble, silt/ sand, gravel, bedrock, wood) at 11 objectively selected locations, but not deeper than 0.5 m, along with hydrological parameters (USEPA 2017). These additional samples were not included in the statistical analyses.

For LM and SEM observations, the preserved diatom samples were oxidized with 30% hydrogen peroxide and heated on hot plate for three hours to remove the organic matter (Stancheva *et al.* 2015). Afterwards, the diatoms were rinsed repeatedly with distilled water to neutrality and mounted in Naphrax®. A minimum of 600 diatom valves were identified to species, or to the lowest possible level if species could not be determined. Species relative abundances were then tabulated for the purposes of stream bioassessment. These same slides were re-counted using the new *Planothidium* species designations proposed by Jahn *et al.* (2017), Van de Vijver *et al.* (2018), and Wetzel *et al.* (2013, 2019). *Planothidium* taxa were identified to species level and quantified both in valve and girdle views based on the best taxonomic approximation for the girdle views and following Krammer & Lange-Bertalot (1991), Bąk & Lange-Bertalot (2014) and Wetzel *et al.* (2014). *Planothidium* taxa were described by observing at least 40 SV and 40 RV valves, except for a few rare species observed in less than five sites. Striae density was determined at the central part of the valve face between valve sternum and margins.

Light microscopy analysis and imaging of the specimens were performed using an Olympus® BX41 Photomicroscope (Olympus America Inc., Center Valley, Pennsylvania) with differential interference contrast optics and an Olympus®

SC30 Digital Camera. Scanning electron microscopy was done on cleaned valves that had been air dried onto cover slips, attached to aluminum stubs, and sputter-coated with 20 nm of iridium. Diatom valves were examined in high vacuum mode using a Zeiss SIGMA 500 (Carl Zeiss Microscopy, Thornwood, NY, USA) at the Nano3 Facility at the University of California, San Diego (La Jolla, CA, USA).

Species-weighted average of environmental variables

Species-weighted averages (WAs) for selected environmental variables, e. g. chloride, conductivity, dissolves organic carbon (DOC), total nitrogen (TN) and total phosphorus (TP) were calculated for the eleven most common species, recorded in minimum of nine sites. Samples with missing data for an environmental variable were omitted. All of these environmental variables were found to be strongly positively skewed, and they were thus log-transformed to reduce the influence of outliers on the calculation of weighted averages (specifically, the log base 10 of data values plus 1 were used; adding 1 avoided mathematically undefined values for environmental variable measurements of 0). Species relative abundances were then used to calculate weighted averages of the environmental variables for each species; relative abundances for a species were multiplied by environmental variable values and the products were summed to produce weighted averages of the environmental variable for that species. Even though a single environmental measurement was available for each sample, the differences in relative abundance of species produced different means for species that had an identical pattern of presence and absence among the samples, and provided a more sensitive assessment of their different environmental associations than would a simple average of sites where the species were found.

All statistical analyses were done with log-transformed environmental data, and then results were back-transformed for interpretation. Arithmetic averages calculated on a log scale are geometric averages on the original linear scale of the data, and thus all of the weighted averages presented are geometric species-weighted averages, rather than arithmetic species-weighted averages.

Randomization test

Because the same set of environmental measurements was used to compare any two species from the dataset, the data were not independent between the species. Dependent samples are often analyzed using paired methods, such as paired t-tests. However, traditional paired analysis would not be an appropriate method for these data, because paired tests compare differences between paired samples against a mean difference of 0. Species that differ in mean along an environmental gradient will have primarily positive differences at one end of the gradient and primarily negative differences at the other, which would average to 0 even though the species differed in their distributions. For traditional paired analysis to be effective, pairs of measurements must have differences that are either consistently positive or consistently negative, which is not expected for data on species with different environmental associations. Therefore, instead of a traditional paired analysis, randomization tests were used to compare the species-weighted environmental averages between pairs of species. Randomization tests are nonparametric methods that lack distributional assumptions (such as normality and homogeneity of variances), and are able to give valid p-values in the face of non-independent data, because the dependencies are incorporated into the randomization procedure.

Each test was a comparison between a pair of species. For a given pair of species, samples in which at least one of the two species was present were selected. Samples in which both species were absent were often well outside of the range of environmental data values used by the species, and those samples were likely to be outside of the niche dimensions for both species. The observed amount of difference between species-weighted averages was calculated and recorded as the test statistic. Then, the environmental variable was randomly shuffled with respect to the species abundance, and new weighted averages were calculated for each species based on the shuffled data. The difference between the species-weighted averages for the shuffled data was calculated and recorded as one of the differences that could be produced at random with these data. This randomization procedure was repeated 100,000 times, and the number of times that the randomly shuffled differences were as big or exceeded the size of the observed difference was determined. The number of random shuffles that exceeded the observed value were then divided by the number of random shuffles, resulting in the p-value for the test. This procedure was repeated for each pair of species and each variable.

Results

Planothidium species diversity

We recorded twenty *Planothidium* species in studied streams and rivers in California, including a species that is new to science. Valve morphology of each species is illustrated with LM photomicrographs. SEM observations are provided for species that are difficult to classify, morphologically variable, rare, or that are little known or new to science. Table 1 summarizes species size ranges, striae density, LM and SEM figures, and main taxonomic references followed. Brief taxonomic notes for each species are provided in the text.

TABLE 1. List of *Planothidium* taxa, recorded in streams and rivers in California*,* including size ranges, striae density, LM and SEM illustrations, and taxonomic references. Abbreviations: (N) number of samples where species was recorded out of 208 samples from wadeable streams used in statistical analysis, (*) species was recorded only in additional samples from non-wadeable rivers, (NA) not available.

Taxon	N	Width	Length	SV striae in 10 µm	RV striae in 10 µm	LM Figure	SEM Figure	Taxonomic References
Species with a sinus								
P. lanceolatum	163	4.5–8.5	10–30	12–14	12–15	1, 2, 6	5, 9, 10, 72	Vijver *et al.* 2013, Jahn *et al.* 2017
P. cryptolanceolatum	57	4.8–7.4	15.1–27.3	11.0–14.5	11.0–14.5	3, 4, 7, 8	11–13	Jahn *et al.* 2017
P. amphibium	33	5–6.7	11–21	13–16	13–16	14–28	29–38	Wetzel *et al.* 2014
P. californicum, sp. nov	2	5.5–7.5	10.4–20.2	15–18	15–18	45–54	39–44	This study
Species with a cavum								
P. frequentissimum	172	3.5–5.8	5–23	13–15	13–15	57–59	55, 56, 68, 70, 71	Jahn *et al.* 2017
P. victorii	57	3.6–7.3	5.1–24.6	11.5–17	11.5–17	62–64	60, 61	Jahn *et al.* 2017
***Planothidium* sp. 1**	14	4–5	10.8–16	13–15.5	13–15.5	65, 66	67, 69	This study
P. rostratoholarcticum	1	3.7–4.6	6.3–11.7	13–18	13–18	73–76	NA	Bąk & Lange-Bertalot 2014, Wetzel *et al.* 2019
P. potapovae	9	5–6	11–17.5	11–13	11–13	78–80	81, 82	Wetzel *et al.* 2019
P. hinzianum	1	5.2–6.0	10.5–14	15–16	15–16	83, 84, 86–91	85	Wetzel *et al.* 2019
P. sheathii*	2	6.3–8.8	14–29	11–13	11–12	92–95	NA	Stancheva 2019
P. incuriatum*	3	6.5–7.1	21–26	12–14	12–15	96–99	NA	Wetzel *et al.* 2013
P. tujii*	1	4.7–5.1	13.3–14.3	16	16	100–103	NA	Wetzel *et al.* 2019
Species without a sinus or cavum								
P. minutissimum	20	3.4–4	8–9.8	14–16	14–17	104–107	NA	Morales 2006, Bąk & Lange-Bertalot 2014
P. granum	4	3.6–4.2	7–9	15–17	15–17	108–111	NA	Morales 2006, Cantonati *et al.* 2017
P. daui*	1	3.6–5.8	7–13	14–17	14–17	112–115	NA	Morales 2006, Cantonati *et al.* 2017
P. engelbrechtii	41	3.3–5.2	6.2–20	16.5–20	16.5–20	116–133	134–147	Compère & Van de Vijver 2009
P. delicatulum	15	5–6.8	10.3–18	13–15	14–16	148–161	166–171	Van de Vijver *et al.* 2018
***Planothidium* sp. 2**	1	4.6–5	10–12	16	16–18	162–165	NA	This study
P. robustum	61	5.8–9.1	12.5–24	13–15	14–16	172–186	187–192	Hustedt 1934, Lange-Bertalot & Krammer 1989

Species with a sinus

Planothdium species belonging to this group are characterized by a presence of unilateral sinus (single horse-shoe shaped mark) on SV, and similar multiseriate striae radiate throughout on both valves. The central SV striae are composed of 3(2–4)rows of areolae, middle row is often shorter and with smaller areolae (Fig. 37), while the central RV striae have 3–4 rows of same sized areolae (Fig. 38). The species within this group are separated morphologically based on a combination of 1) sinus outline and degree of development (i.e. deep vs. shallow), and 2) valve size and outline. The striae density significantly overlaps between similar species and thus cannot be used as distinguishing feature.

Planothidium lanceolatum (Brébisson ex Kützing) Lange-Bertalot 1999

The valves are lanceolate to elliptical-lanceolate with slightly drawn out apices (Figs 1, 2, 5, 6, 9, 10). The SV has a linear-lanceolate axial area with a unilateral circular rimmed depression on the internal valve surface (sinus) and a slightly reduced stria on the opposite side (Figs 1, 2, 6, 9, 10). The RV has 2–5 shortened striae (Fig. 72) beside the central area according to Jahn *et al.* (2017), but 1–3 striae according to van de Vijver *et al.* (2013).

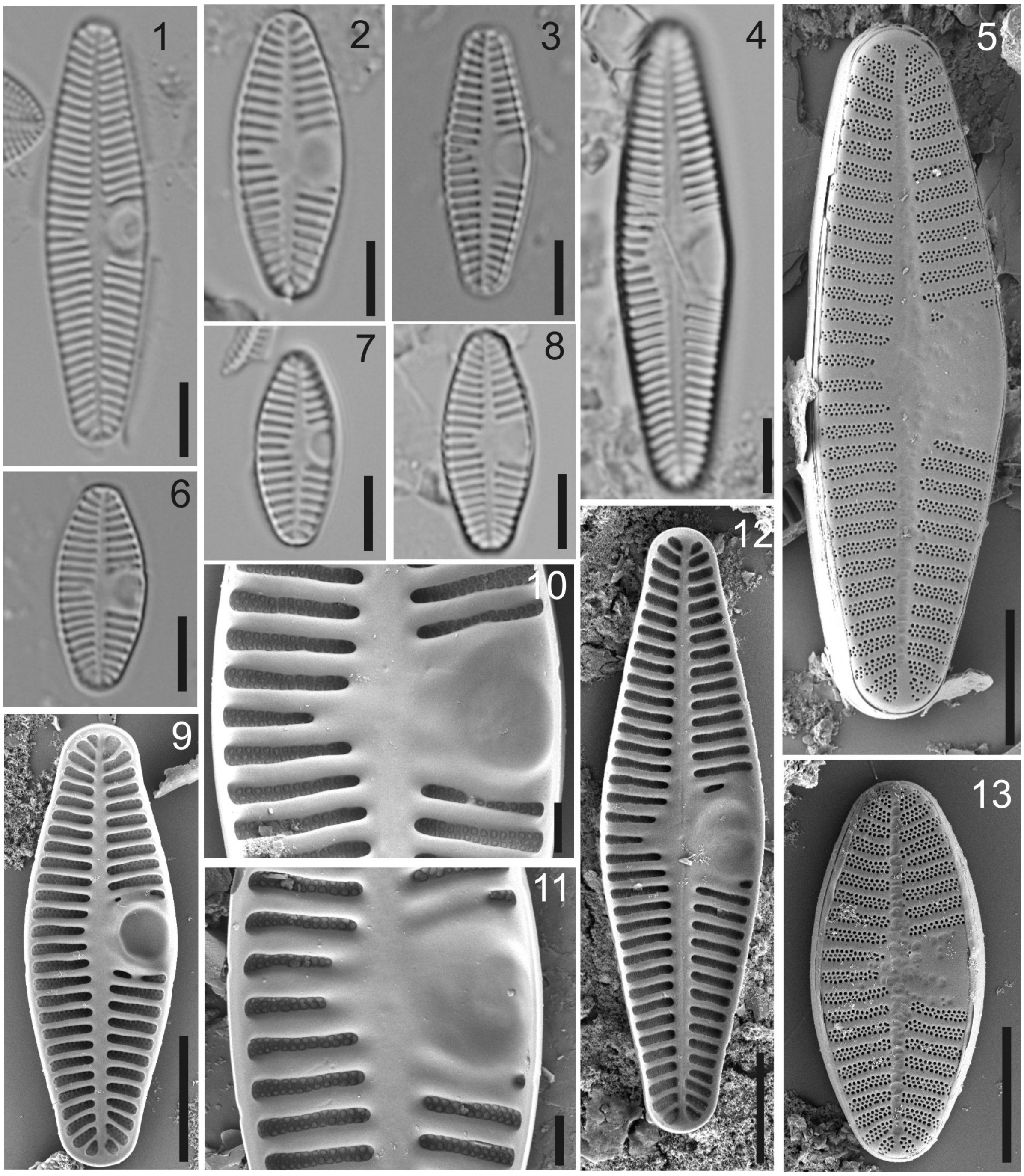

FIGURE 1–13. *P. lanceolatum* (1, 2, 5, 6, 9, 10) and *P. cryptolanceolatum* (3, 4, 7, 8, 11, 12, 13) LM and SEM. Samples: 403M05757 (1), SMC09698 (2, 6, 8, 4, 10, 11), 534PS0134 (5, 9, 12, 13), 905WE0679 (3), 106PS0270 (7). Scale bars: 5 µm (1–9, 12, 13), 1 µm (10, 11).

SEM: SV striae with 3–4 rows of small areolae continue onto the valve mantle, with merged 1–3 areolae offset from the valve striae (Figs 5, 9, 10). RV striae with 3–4 rows of small areolae on valve face (Fig. 72).

Comments: This species was lectotypified by Van de Vijver *et al.* (2013) and redefined by Jahn *et al.* (2017).

***Planothidium cryptolanceolatum* R. Jahn & N. Abarca 2017**

This species differs from *P. lanceolatum* by its slender asymmetric valve outline (Figs 3, 4, 7, 8) and by a smaller, shallower and irregularly half-moon shaped sinus with a deeper hemicircular depression at the mantle (Figs 11, 12). The RV has 1–3 shortened striae beside the central area.

SEM: SV striae with 2–3 rows of small areolae continue onto the valve mantle, with merged 2–3 areolae offset from the valve striae (Fig. 13). RV striae with 3–4 rows of small areolae on valve face.

Comments: This species was identified strictly after Jahn *et al.* (2017). The most reliable discriminating feature between *P. lanceolatum* and *P. cryptolanceolatum* seems to be the size and form of the sinus (Jahn *et al.* 2017). Indeed, transitional sinus morphology complicated the separation of both species during the routine LM identification. Additional LM discriminating feature, such as the shortened striae beside the central area on RV, seems to overlap in both species frequently.

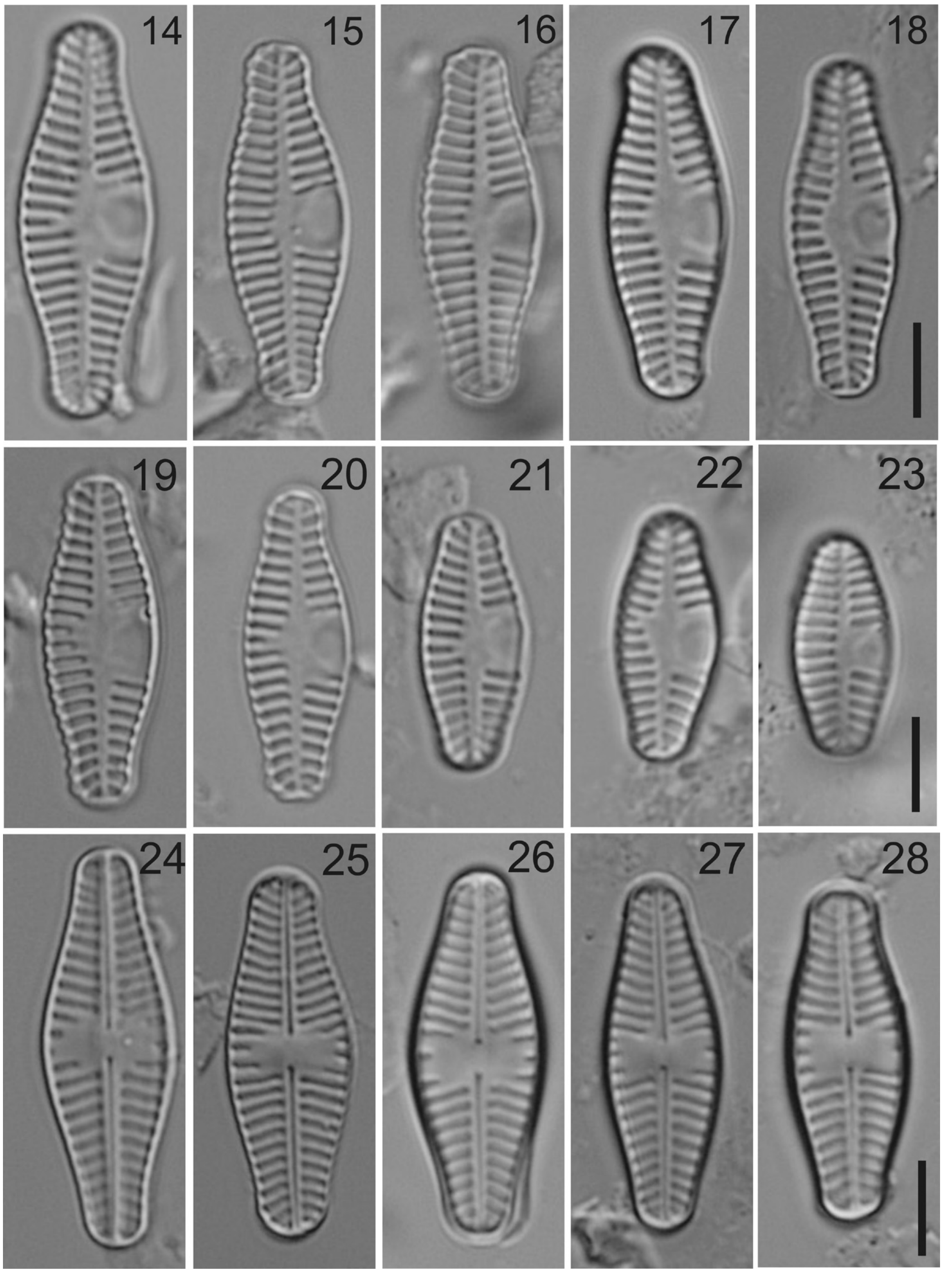

FIGURE 14–28. *P. amphibium* LM. All images are from sample 903NP9SLR. All scale bars: 5 µm.

Planothidium amphibium C. E. Wetzel, L. Ector & L. Pfister 2014

The valves are linear to linear-lanceolate with capitate to subcapitate, protracted apices (Figs 14–36). The SV has a prominent oval or half-moon sinus variable in depth, with circular or hemicircular depression (Figs 14–23, 36).

SEM: SV striae with 3 to 4 rows of areolae, middle row is often shorter and with smaller areolae (Fig. 29–32, 37). The SV striae continue onto the valve mantle, with merged 3–4 areolae offset from the valve striae (Fig. 32). RV striae with 3–4 rows of small same sized areolae on valve face (Figs 33–35, 38).

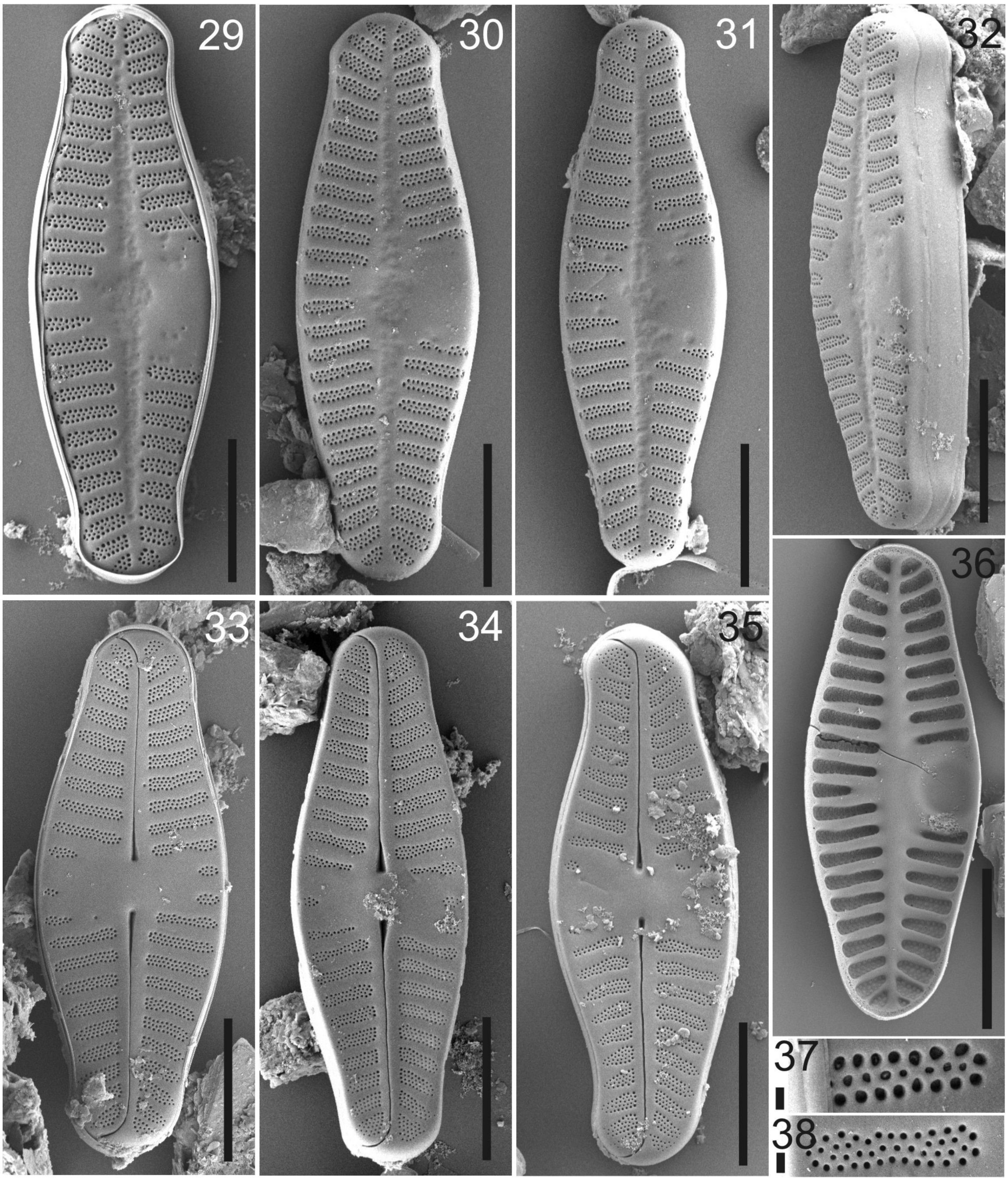

FIGURE 29–38. *P. amphibium* SEM. All images are from sample: 901NP9LCC. Fig. 37 shows detail of SV striae, and Fig. 38—detail of RV striae. Scale bars: 5 µm (29–35), 200 nm (37, 38).

Comments: This species agrees well with original description (Wetzel *et al.* 2014), except for the slightly wider valves being up to 6.7 µm. The discriminating features from *P. lanceolatum* and *P. cryptolanceolatum* are the capitate to subcapitate, protracted apices in *P. amphibium*, and the shape of sinus, which can vary from oval to half-moon. Although the valve dimensions and striae number overlap, *P. amphibum* has smaller valves and denser striae than *P. lanceolatum*. This species was previously reported as *P. haynaldii* in the USA (Potapova 2011). However, *P. haynaldii*, which is a rare species distributed in the Andes Mts. of South America (Ecuador, Chile) has wider and more strongly bent valves (Wetzel *et al.* 2014). We did not record *P. haynaldii* in studied streams in California.

Planothidium californicum **Stancheva & N. Kristan, *sp. nov.* (Figs 39–54)**

Valve outline and dimensions: The valves are elliptic-lanceolate with slightly drawn out apices, 5.5 to 7.5 µm wide, 10.4–20.2 µm long, striae 15 to 18 in 10 µm on both valves.

LM of SV (Figs 45, 47–49, 53, 54): The axial area is narrow and linear. The central area on one side with a distinctly rimmed, oval or half-moon to triangular shaped sinus, often surrounded by 1–2 very short incompletely developed striae (Figs 45, 48, 49, 53). The opposite side of central area bordered by 1–2 slightly shortened striae. The striae are radiate throughout the valve.

LM of RV (Figs 46, 50–52): The axial area is narrow, linear. The central area forms a rectangular unilateral fascia, with 2–3 shorter striae on one side and lacking central striae on the opposite side. Striae radiate throughout the valve.

SEM of SV (Figs 40, 41, 43, 44): The striae with two rows of areolae, with a possible third short row present near the margin, the areolae of the middle row are markedly smaller (Figs 40, 43). Striae continue some distance onto the mantle and one to three areolae on the mantle are offset from the valve striae (Fig. 43). Internally, SV striae are separated by thick virgae (Fig. 41). The sinus is pronounced, deep, and oval to triangular in shape, distinctly rimmed, and surrounded by a raised ridge (Figs 41, 44).

SEM of RV (Figs 39, 42): The striae are comprised of 3 to 4 rows of same sized areolae (Fig. 39, 42). Internally, each areola is covered by a hymenate occlusion (Fig. 42). The raphe branches are straight; internally the raphe branches are weakly deflected to opposite sides (Fig. 39). External RV view was not observed due to low abundance of this species.

Type locality: USA, California, Clark Fork of Disaster Creek (534PS0134), Sierra Nevada Mts, Stanislaus National Forest, 38.41167, -119.76316, altitude 1958 m, collector Jennifer York, *June 16, 2015.*

Holotype: Slide GC 65336 at the Academy of Natural Science of Drexel University Diatom Herbarium, Philadelphia, USA. The holotype specimen is illustrated on Fig. 45.

Isotype: Slide RS! 18 and cleaned material at CSUSM, USA.

Etymology: The epithet refers to the USA state of California, where the species was first observed.

Distribution and ecological notes: The stream type locality is characterized by pH 6.1 and low nutrients (TN <0.03 mg/L, TP <0.02 mg/L), DOC (0.87 mg/L), conductivity (43.8 µS/cm), and chloride (0.37 mg/L). *P. californicum* co-occurred in Clark Fork of Disaster Creek with another recently described species from the Sierra Nevada Mts, i. e. *Gomphonema californicum* Stancheva & Kociolek (Stancheva *et al.* 2016). *P. californicum* was also observed as rare in Hat Creek (526PS1724) in the Lassen National Forest in the Southern Cascade Mts, which is a type locality for new *Cocconeis cascadensis* Stancheva (see Stancheva (2019) for site description).

Comments: *P. californicum* is most similar to *P. taeansa* R. Jahn & N. Abarca, described from a creek in Korea and so far known only from the type locality (Jahn *et al.* 2017). Both species share similar valve outline and striae ultrastructure, but *P. taeansa* differs in: 1) larger cells, which are proportionally longer; 2) lower striae number (12.5–13 in 10 µm); 3) less pronounced, shallower, slightly rimmed sinus; 4) RV with symmetrical central area shaped by 2–3 short striae on both sides. *P. californicum* is similar in valve shape, size and sinus outline to *P. dubium* (Grunow) Round & L. Bukhtiyarova and *P. reichardtii* Lange-Bertalot & Werum. However, both species differ in having SV striae with 3 to 4 rows same sized areolae and less pronounced sinus (Lange-Bertalot & Krammer, 1989, Plate 91, Figs 3–5; Potapova 2011, Werum & Lange-Bertalot 2004, Plate 15: Figs 17, 18).

Species with a cavum

Planothdium species belonging to this group are characterized by a presence of unilateral cavum (double horse-shoe shaped mark) on SV, and similar multiseriate striae radiate throughout on both valves, composed of same sized areolae, organized in up to 4 rows in most taxa, and up to 5 rows in two of the species. The species within this group are separated morphologically based on combination of the outline and size of the valve, the cavum and its opening. The striae density significantly overlaps between similar species and cannot be used as distinguishing feature for most of the species.

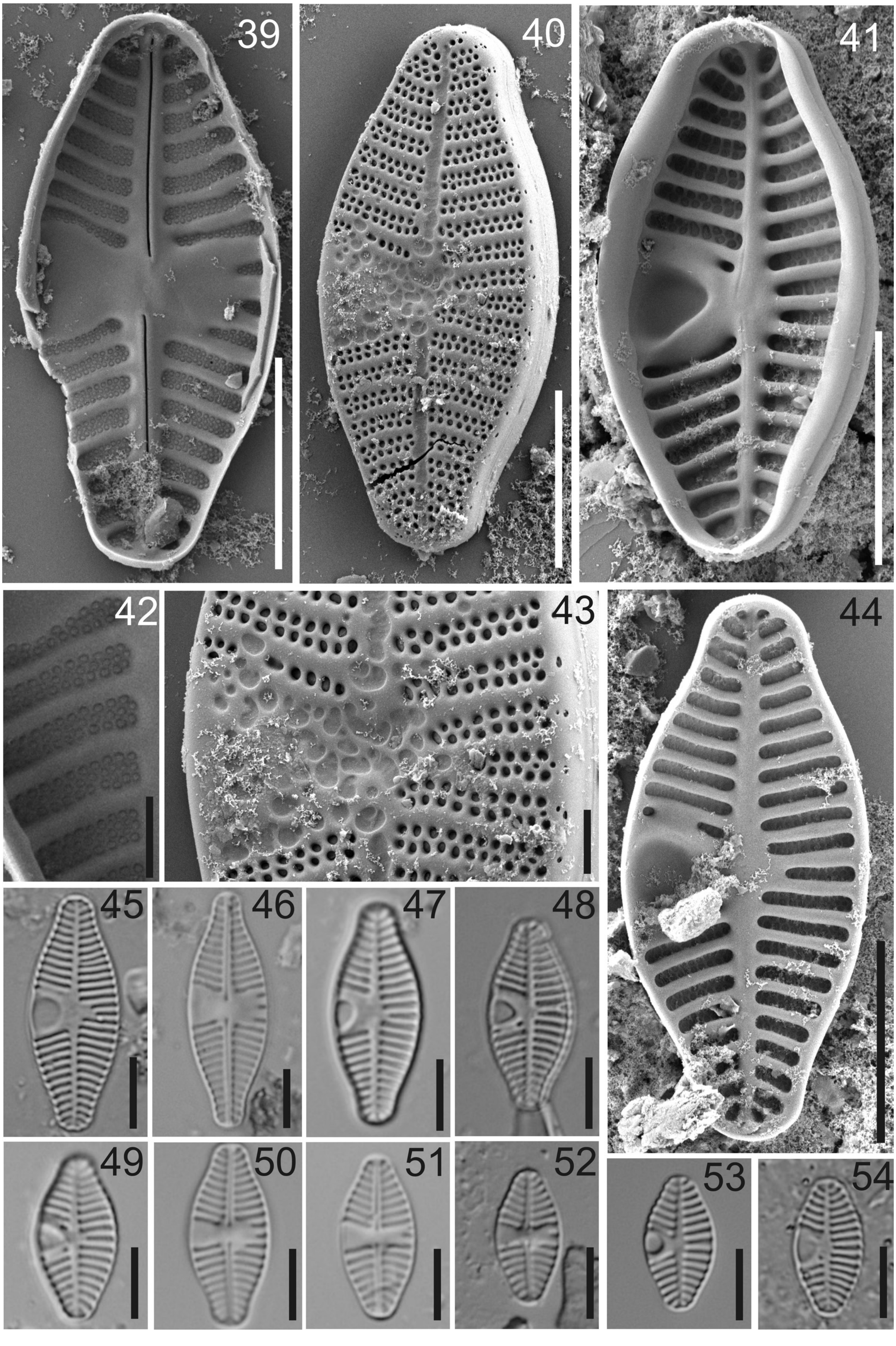

FIGURE 39–54. *P. californicum* Stancheva & N. Kristan, *sp. nov*. SEM images: Fig 39, 42—internal RV view; Figs 40, 43—external SV view; Figs 41, 44—internal SV view. LM images: Figs 45, 47–49, 53, 54—SV; Figs 46, 50–52—RV. Fig. 45 = holotype. Samples: 534PS0134 (39–49, 51–54) and 526PS1724 (50). Scale bars: 1 µm (42, 43); 5 µm (39–41, 44–54).

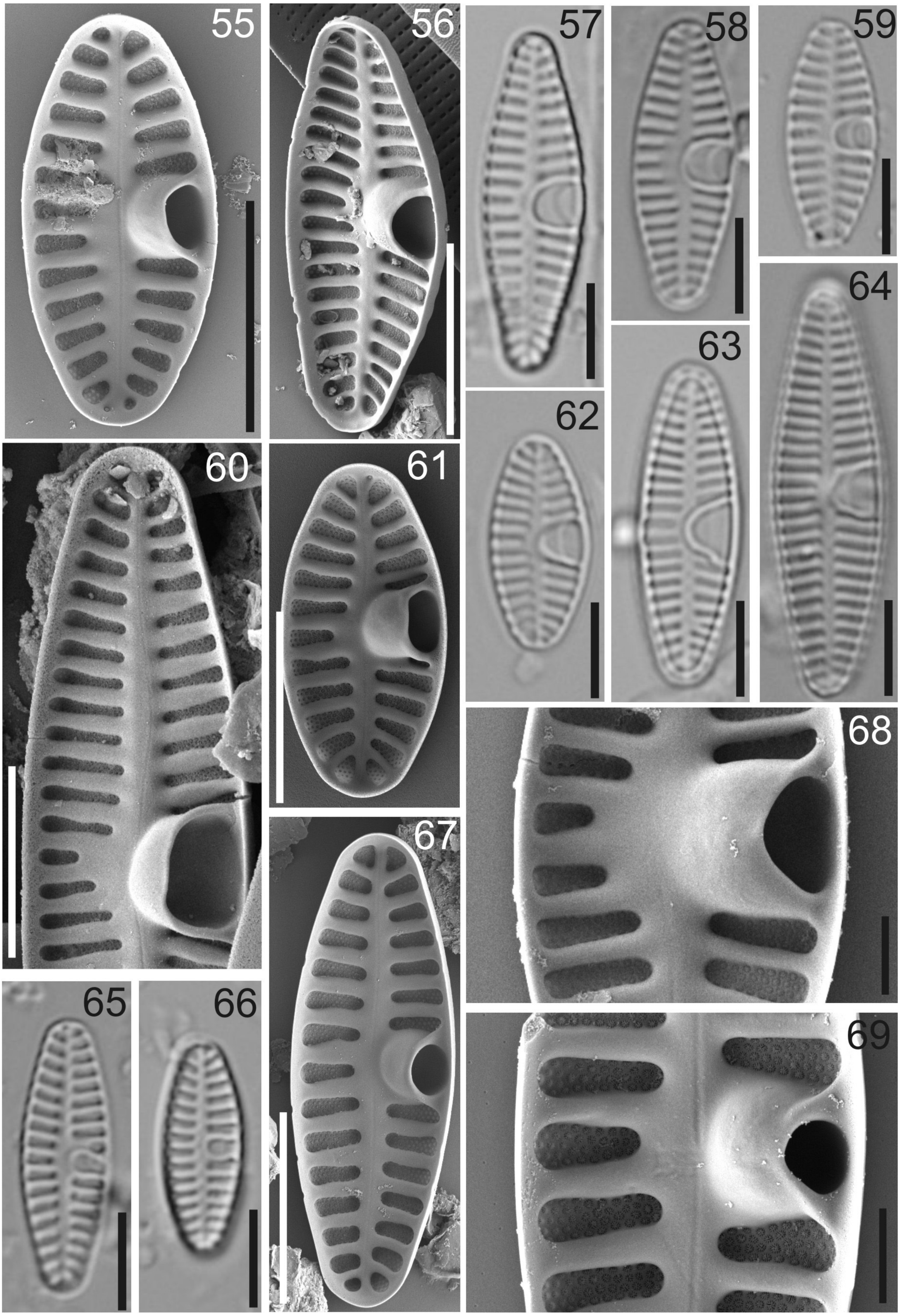

FIGURE 55–69. *P. frequentissimum* (55–59, 68), *P. victorii* (60–64), *Planothidium* sp. 1 (65–67, 69) LM and SEM. Samples: 906M23302 (60, 61); 534PS0134 (68); SMC09698 (56, 57); 901BELOLV (55, 65–67, 69), 205PS0298 (62, 58), SMC16169 (59), 519PS0706 (63), 902M20173 (64). Scale bars: 1 µm (68, 69); 5 µm (55–67).

Planothidium frequentissimum **(Lange-Bertalot) Lange-Bertalot 1999**

The valves are lanceolate to elliptic-lanceolate with rounded or slightly protracted apices (Figs 55–59). The SV has a linear-lanceolate axial area with a unilateral small rounded cavum with parallel sides (Figs 57–59) and a narrow opening (Figs 55, 56, 68) visible in LM as a curved line close to the mantle (Figs 57–59). RV has 1–5 shortened striae beside the central area (Fig. 71).

SEM: The striae on both valves are composed of 3–4 rows of areolae (Figs 55, 56, 70, 71).

Planothidium victorii **P. M. Novis, J. Braidwood & C. Kilroy 2012**

This species differs from *P. frequentissimum* mainly by the shape of the cavum and its opening (Jahn *et al.* 2017). The cavum is V-shaped (Figs 62–64) with a wide and uneven opening (Figs 60, 61), seen as an almost straight line further from the mantle under LM.

Planothidium **sp. 1**

The valves are elliptic-lanceolate with rounded apices (Figs. 65–67). The SV has a narrow linear axial area and unilateral narrow cavum with small pinched opening (Figs 67, 69); central striae on the opposite side are not or very slightly shortened (Figs 65–67). RV has 2–3 shortened central striae on both sides of central area.

SEM: The SV striae are composed of 4–5 rows of areolae (Fig. 69), appearing thicker in LM than the striae in *P. frequentissimum* and *P. victorii*, which have 3–4 row of areolae.

Comments: This species is easy to distinguish from *P. frequentissimum* and *P. victorii,* based on its roundish apices, smaller cavum with very narrow opening and thicker striae. *Planothidium straubianum* C. E. Wetzel, B. Van de Vijver & L. Ector has more elliptical valves, which are proportionally shorter, and 1 to 3 short striae opposite to the cavum. Cavum with similar outline is characteristic for *Planothidium aueri* (Krasske) Lange-Bertalot as well. This taxon was rare in studied data set and needs more observations.

Planothidium rostratoholarcticum **Lange-Bertalot & Bąk 2015**

The valves are elliptical, with broadly protracted to subrostrate apices (Figs 73–76). The SV has a narrow linear axial area. The central area has a unilateral large cavum; on the opposite side, the central striae are not shortened and reach the axial area (Fig. 76) or the central stria indistinctly shortened (Figs 73, 74). The RV has a narrow linear axial area and irregular central area bordered by one or two shortened striae on each side (Fig. 75).

SEM: According to Bąk & Lange-Bertalot (2014) and Wetzel *et al.* (2019), the striae on both SV and RV are similar, with 2 to 3 (rarely 4) rows of same sized areolae on valve face.

Planothidium potapovae **C. E. Wetzel & L. Ector 2019**

The valves are lanceolate to broadly elliptic-lanceolate, with distinctly rostrate apices (Figs 78–82). The SV has a linear-lanceolate axial area, broadening considerably towards central area, which has unilateral prominent cavum and shortened central striae on opposite side (Figs 79, 80). RV with narrow linear axial area and rectangular central area bordered by one to three shortened striae on each side (Fig. 78).

SEM: The SV striae are composed of four to five rows of small same sized areolae (Fig. 81, 82). The striae continue onto the valve mantle in groups of up to eight small areolae. The valve exterior surface is strongly marked with irregular lines along the axial and central area (Fig. 82). The internal SV shows a prominent cavum with a large opening (Fig. 81).

Comments: Wetzel *et al.* (2019) provided a clear concept about three similar species, i.e. *P. rostratocholarcticum*, *P. rostratum* (Østrup) Lange-Bertalot and *P. potapovae*. *P. potapovae* is separated from *P. rostratocholarcticum* and *P. rostratum* based on its distinctly wider central area on SV and striae composed of up to five areolae, particularly on the valve mantle. Furthermore, the SV striae in *P. rostratum* are composed of areolae of different size, the middle two rows are smaller on valve face, and at least one areolae is elongated on mantle.

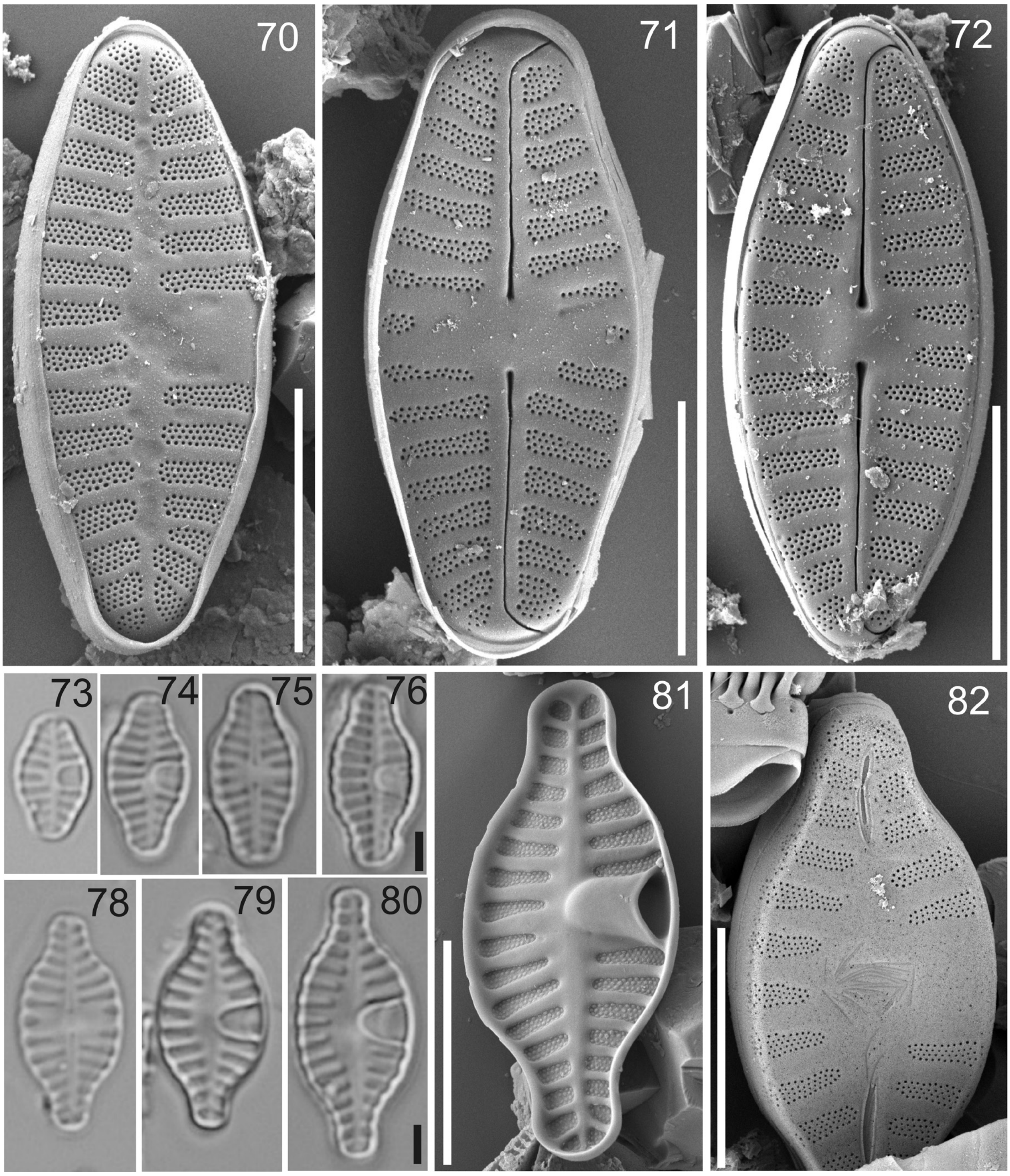

FIGURE 70–82. *P. frequentissimum* (70, 71)*, P. lanceolatum* (72), *P. rostratoholarcticum* (73–76), *P. potapovae* (78–82) LM and SEM. Samples: 901NP9LCC (70, 71), 534PS0134 (72), 105PS1564 (73–82). Scale bars: 5 µm (70–72, 81, 82); 2 µm (73–76, 78–80).

Planothidium hinzianum C. E. Wetzel, B. Van de Vijver & L. Ector 2019

The valves are elliptic-lanceolate with acutely rounded ends (Figs 83–91). The SV has a lanceolate axial area broadening asymmetrically to a central area with unilateral prominent cavum with large hood opening linked to the neighboring striae (Figs 84, 86, 87, 90, 91). The RV has a narrow linear axial area and transapically expanded central area bordered by one or two short central striae on each side (Figs 84, 89).

SEM: Only an external SV was observed (Fig. 85). The striae are conical, composed of 4 to 5 rows of same sized areolae, tapering to 2–3 rows near the tips. Striae continue some distance onto the mantle, forming groups of 4 to 8 areolae, which are offset from the valve striae; two peripheral areolae are elongated with linear openings. According to Wetzel *et al.* (2019), the RV striae are composed of three rows of areolae with fourth short row inserted near the mantle.

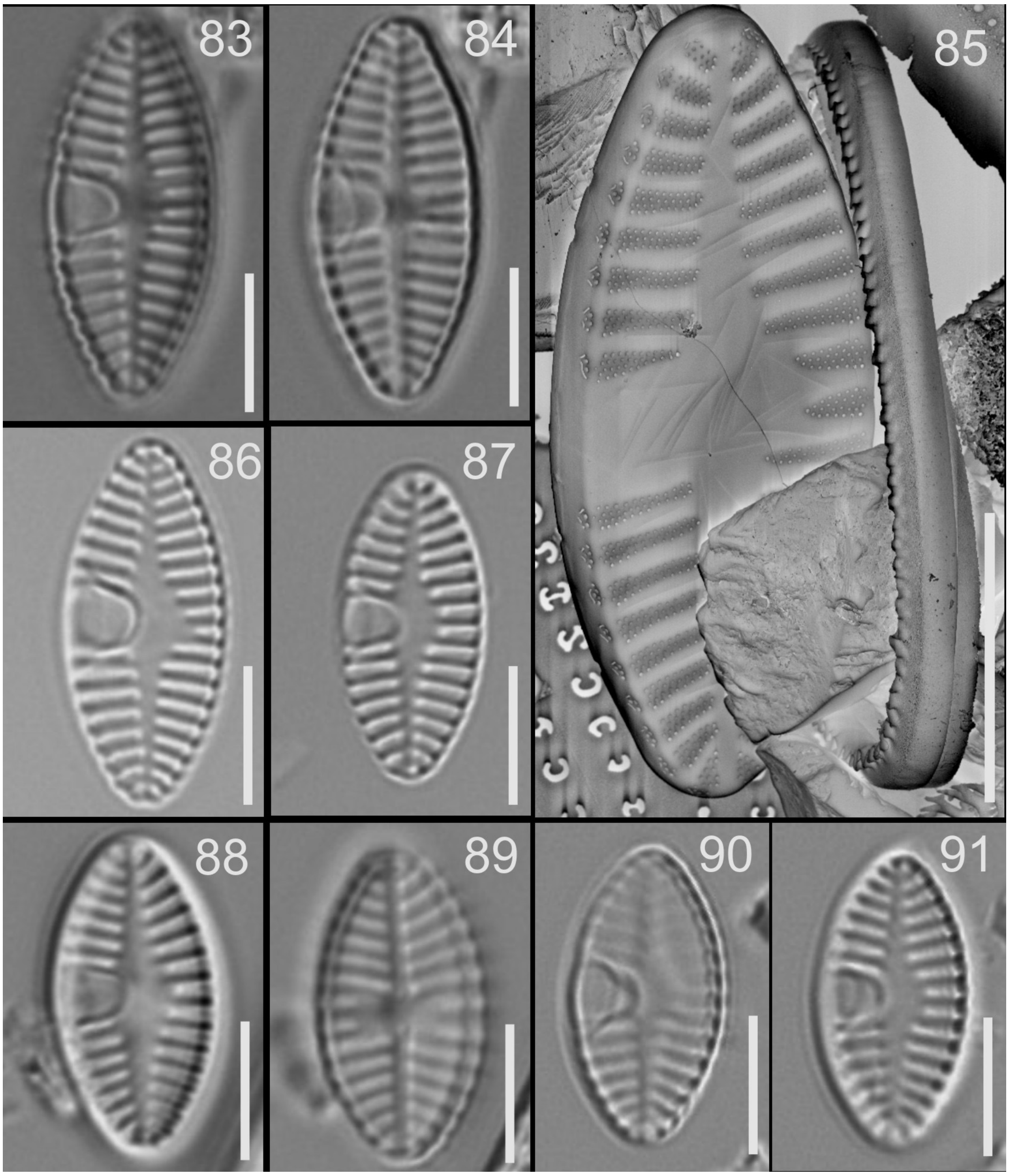

FIGURE 83–91. *P. hinzianum* LM and SEM. Sample: 105PS0295. All scale bars: 5 µm.

Comments: The ultrastructural observations of this species are insufficient, due to its rarity. *P. hinzianum* should be compared with *P. sheathii,* recently described species from California (Stancheva 2019), which differs by larger and more elliptical valves with lower striae density (Figs 92–95). Furthermore, the striae in *P. sheathii* on both valves contain more rows of areolae (up to 6 rows) and form larger groups of areolae on the mantle.

Planothidium sheathii **Stancheva 2019**

The valves are broadly lanceolate to elliptical with obtusely rounded apices (Figs 92–95). The SV has a narrow, lanceolate axial area that expands slightly towards the central, and contain unilateral prominent oblong cavum with broad hood opening which reaches the neighboring striae (Figs 92–94). The RV has a very narrow, linear axial area with a rectangular central area bordered by 2–3 shortened striae (Fig. 95).

SEM: According to Stancheva (2019), the striae on both SV and RV are composed of 4 to 6 rows of same sized areolae, and continue some distance onto the mantle, forming groups of 8 to 15 areolae, which are offset from the valve striae; two peripheral areolae on SV are elongated with linear openings.

Comments: This species is larger and coarser than *P. hinzianum* and has different valve outline (see above).

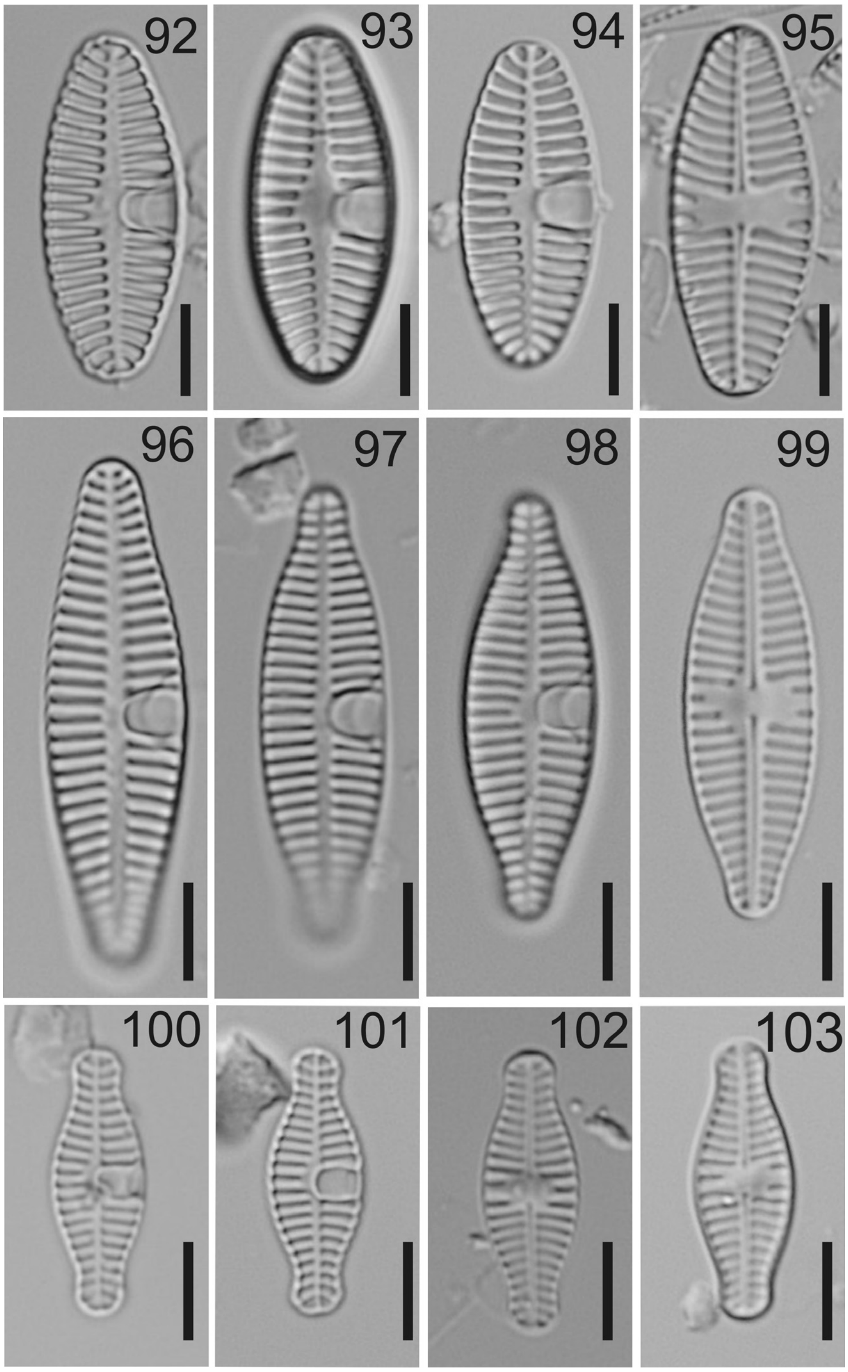

FIGURE 92–103. *P. sheathii* (92–95), *P. incuriatum* (96–99), *P. tujii* (100–103) LM. Samples: CA10056 (92–95), CA10020 (96–103). All scale bars: 5 µm.

Planothidium incuriatum **C. E. Wetzel, Van de Vijver & L. Ector 2013**

The valves are lanceolate with subrostrate apices (Figs 96–99). The SV has a narrow, linear axial area and unilateral large cavum with expanded internal hood opening. The RV was not captured. The RV has a narrow, linear axial area and variable, transversely rectangular to elliptic central area bordered by 2 shortened striae on each side (Wetzel *et al.*, 2013).

Planothidium tujii **C. E. Wetzel & L. Ector 2019**

The valves are lanceolate with rostrate to capitate apices (Figs 100–103). The SV has a narrow, linear axial area and a horseshoe-shaped cavum with opening but not extending beyond the cavum margins (Figs100, 101). The RV has a narrow linear axial area and rectangular central area bordered by 2 shortened striae on each side (Figs 102–103).

Comments: *P. biporomum* (M. H. Hohn & Hellerman) Lange-Bertalot is easily distinguished with LM by the larger valves, lower striae density and cavum with wide hood opening, which flares out of the cavum margins (Wetzel *et al.* 2013).

Species without a sinus or cavum

Species belonging to this morphological group have multiseriate striae with variable ultrastructure and 2 to 8 rows of areolae per stria. Additional criteria for species identification are: valve outline, dimensions, striae position and length, shape of axial and central areas.

Planothidium minutissimum (Krasske) E. A. Morales 2006

The valves are rhomboidal with blunt or slightly rostrate apices (Figs 104–107). The SV has a narrow, linear axial area that expands into a small, variably shaped central area with 2 central striae separated by a distinctly larger virga on one side (Figs 104–106). The RV has a lanceolate axial area that expands into a small and variably shaped central area with 1–2 shortened striae (Fig. 107). Striae weakly radiate through both valves (Figs 104–107).

SEM: According to Morales (2006) and Bąk & Lange-Bertalot (2014), the striae on both valves are composed of 3 rows of areolae, with shorter incomplete middle row on RV.

Planothidium granum (M. H. Hohl & Hellerman) Lange-Bertalot 1999

The valves are rhomboidal with blunt or short subrostrate apices (Figs 108–111). The SV has a narrow, linear axial area with a weakly defined central area with no shortened striae (Figs 108–110). The RV has a narrow, lanceolate axial area with a small central area with shortened striae on both sides (Fig. 111). Striae weakly to moderately radiate on SV (Figs 108–110) and strongly radiate on RV (Fig. 111).

SEM: According to Morales (2006), RV striae are with 3–5 rows of areolae with narrow depressed virgae, SV striae with 4 or more rows of areolae.

Planothidium daui (Foged) Lange-Bertalot 1999

The valves are lanceolate with drawn out, rostrate to capitate apices (Figs 112–115). The SV has narrow, linear axial area without expanded central area and striae parallel at the center and weakly radiate towards the apices (Figs 112–114). The RV has strongly radiate striae, linear axial area, and rectangular central area with 1 or 2 shortened striae on both sides (Fig. 115).

SEM: According to Morales (2006), SV striae are with 5–8 rows of areolae with narrow depressed virgae, RV striae with 2–6 rows of areolae.

Planothidium engelbrechtii (Cholnoky) Round & L. Bukhtiyarova 1996

The larger valves are lanceolate to elliptic–lanceolate with broadly protracted to slightly rostrate apices (Figs 116–120, 126). The smaller valves are more rhombic–lanceolate with less protracted or rounded apices (Figs 122–125, 128–133). The SV striae are slightly radiate to almost parallel, with a narrow linear (Fig. 130) to linear-lanceolate axial area (Figs 119, 120, 122, 128), a very weakly enlarged central area (Figs 116, 126, 132) which is unilaterally expanded in some specimens due to the shortening of a central stria (Figs 122, 128) or a gap between the central striae (Figs 124, 130). Typically, the mid-and small-sized SV tend to have unilaterally expanded central area with shortened central striae or a gap (Figs 122, 128, 130), compare to larger valves from the same populations with more symmetrical central area (Fig. 126, 132). However, in some populations, a gap or shortened central striae were not observed on the SVs regardless of size diminution (Figs 116–121). The RV has slightly radiate striae, raphe, narrow linear axial area, and enlarged central area slightly unilaterally expanded due to the shortening of one or two central striae (Figs 117, 118, 123, 127, 129, 133).

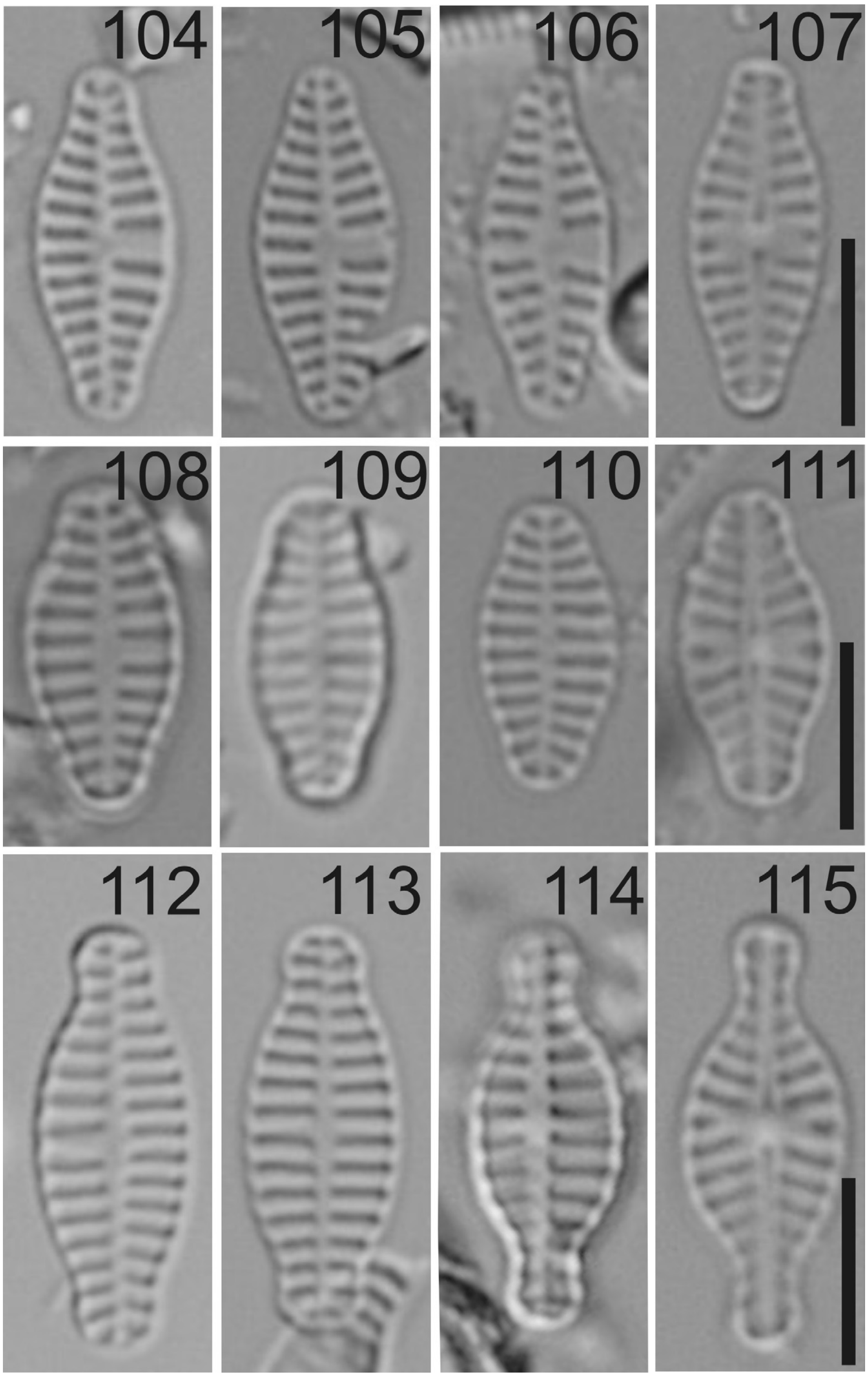

FIGURE 104–115. *P. minutissimum* (104–107), *P. granum* (108–111), *P. daui* (112–115) LM. Samples: 903NP9UAC (104–107), 105PS1564 (108–111), CA10020 (112, 113), CA10028 (114, 115). All scale bars: 5 µm.

SEM: The SV striae have 3 to 4 rows of areolae, separated by slightly raised virgae (Figs 134–140). In the larger valves, SV striae have middle row of smaller areolae (Figs 136, 137), while in the smaller valves areolae appear same sized (Figs 139, 140). RV with 3 rows of areolae with middle row shorter and sometimes with smaller areolae (Figs 141–143).

Comments: Valve dimensions, outline and striae number agree well with *P. engelbrechtii* concept of Cholnoky (1955) and Compère & Van de Vijer (2009), except for a few slightly shorter valves recorded (6.2 µm long). *However, populations of P. engelbrechtii from California, showed variation in the valve outline, striae, axial and central areas, and may represent a complex of species, which is a subject of continuing research.*

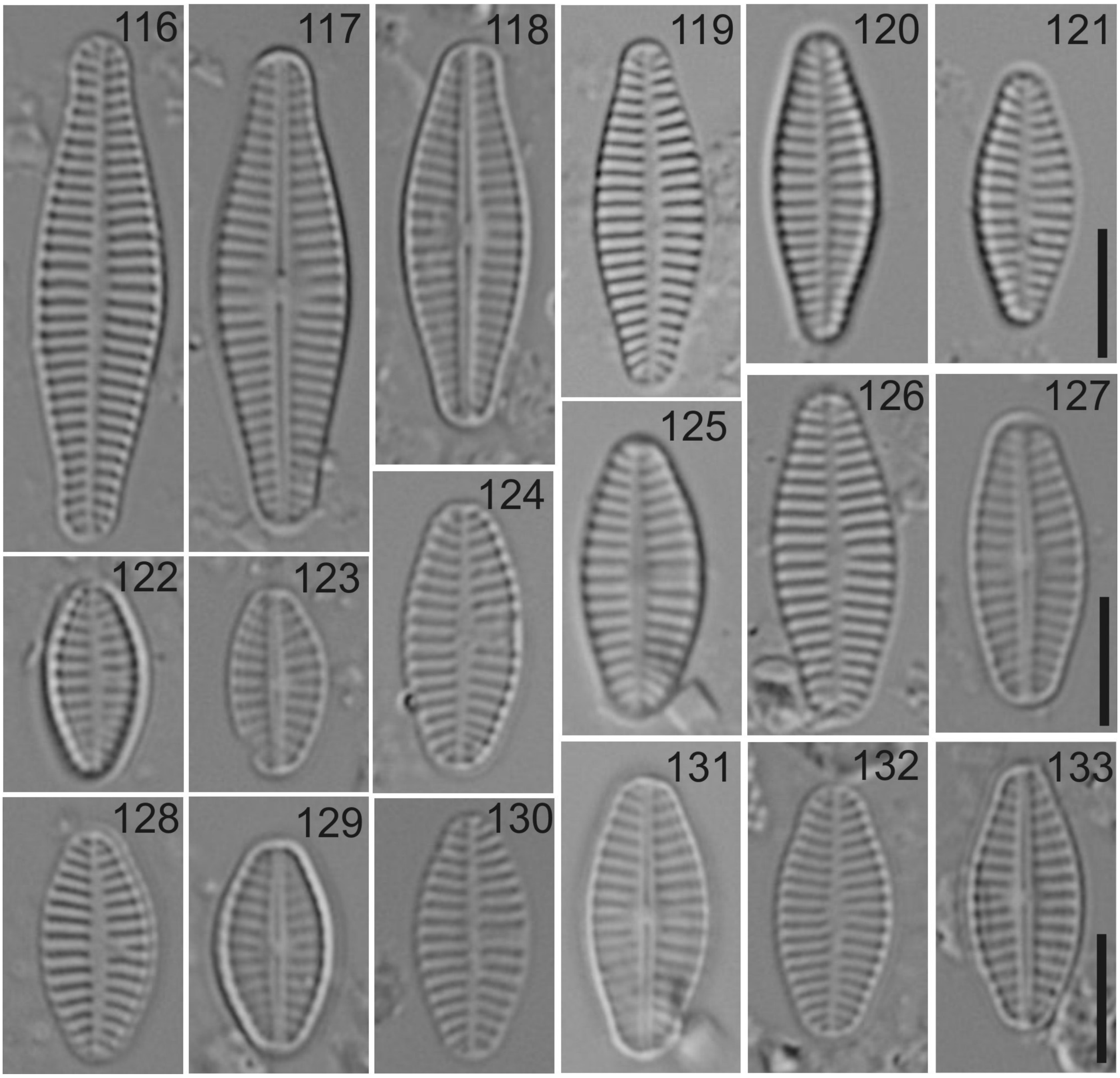

FIGURE 116–133. *P.engelbrechtii* LM. Samples: 903NPSLR (116–121), 906M23302 (128–130, 132, 133), 404M07362 (122–124, 126, 127), 901M14126 (125 and 131 are same frustule). All scale bars: 5 µm.

Another similar species is *P. pericavum* (Carter) Lange-Bertalot, described from the Tristan da Cunha Archipelago (southern Atlantic Ocean) by Carter (1966). It has less protracted valve apices according to Compère & Van de Vijer (2009) and striae composed of only two rows of areolae, as illustrated by Lange-Bertalot & Krammer (1989, Plate 92, Fig. 9). Indeed, recent study of populations of *P. pericavum* from Tristan da Cunha (Van de Vijer *et al.* 2019) showed that the striae ultrastructure of this species and valve dimensions are not distinguishable from *P. engelbrechtii*. Two similar species were recently described from freshwaters in Europe, i.e. *P. galaicum* Álvares-Blanco & S. Blanco (Álvarez-Blanco & Blanco 2013), which has siliceous granules (striae are undiscernible), and *Planothidium lacustre* Álvares-Blanco, Cejudo-Figueiras & S. Blanco (Blanco *et al.* 2013), which differs by bi-seriate striae.

Smaller specimens of *P. engelbrechtii*, if distributed separately from larger specimens (which is not typical in studied streams), should be compared with other small-sized *Planothidium* taxa with similar valve outline and without a cavum or sinus. In general, all comparable small *Planothidium* taxa have lower striae density (less than 17 striae in 10 µm). In addition, *P. granum, P. daui* (Morales 2006), *P. neglectum* Lange-Bertalot & Rumrich (Rumrich *et al.* 2000), and *P. pumilum* (Bąk & Lange-Bertalot 2014) have SV striae with 5–6 or more rows of areolae separated by depressed virgae externally, and *P. werumianum* has a SV with bi-seriate striae and wide lanceolate axial area (Bąk & Lange-Bertalot 2014). The small-sized *Planothidium* species with consistently tri-seriate striae on both valves and could be distinguished from the small specimens of *P. engelbrechtii* as follows: *P. minitissimum*—by rhomboidal valve outline in combination with large unilateral gap, without short central stria on SV and 13–15 striae in 10 µm (Morales 2006), *P. rhombicum* (Bąk & Lange-Bertalot 2014)—by rhomboidal-lanceolate valve outline, lack of unilateral gap, but sometimes short central stria on SV and 12.5–15.5 striae in 10 µm; *P. suncheonmanense* (Jahn *et al.* 2017)—restricted to Korea—by the lack of unilateral gap, but sometimes short central stria on SV and 15–17 striae in 10 µm, as well as virgae not elevated externally as in *P. englelbrechtii*.

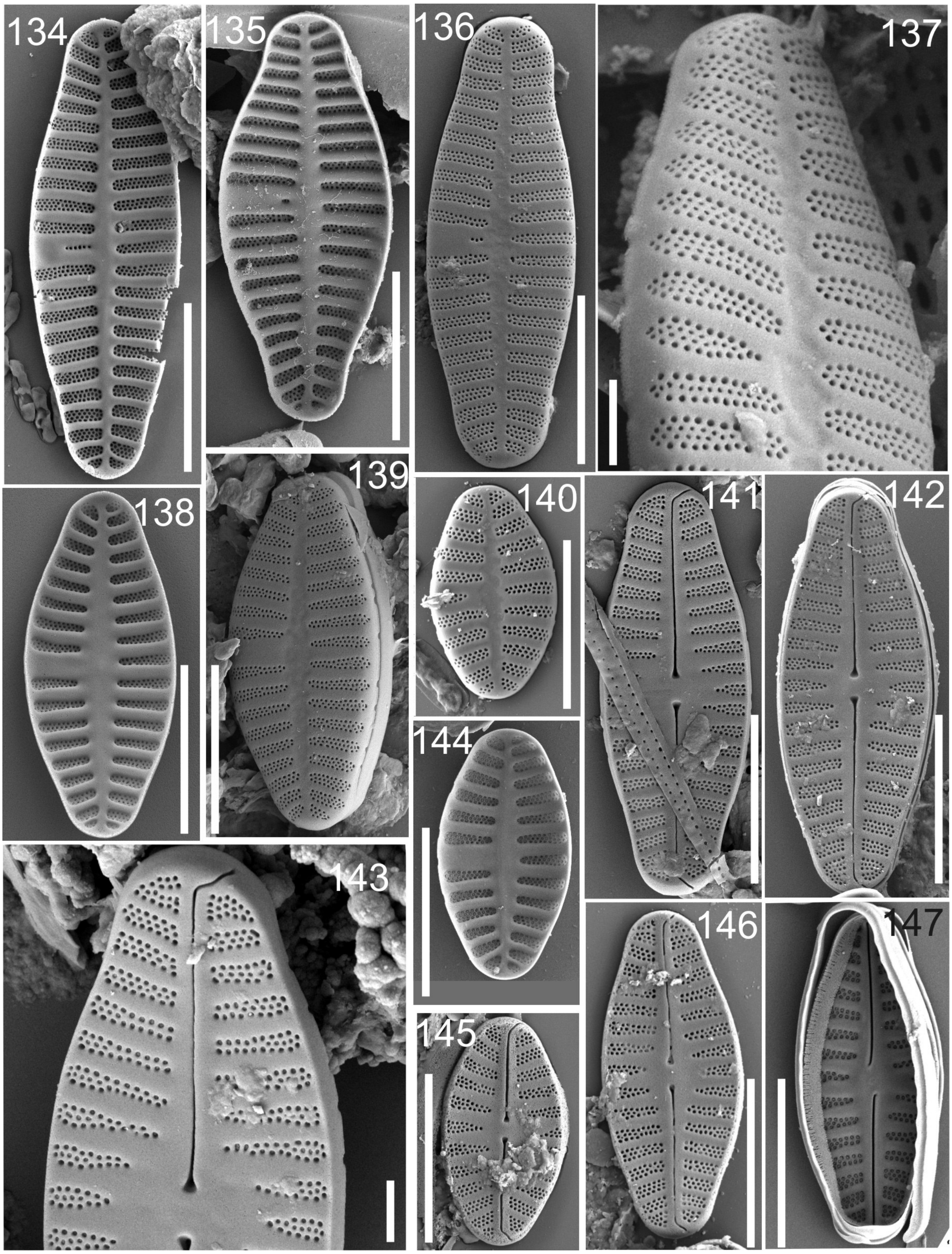

FIGURE 134–147. *P. engelbrechtii* SEM. Samples: 906M23302 (134, 137, 138, 140, 142, 144–147), 404M07362 (136, 139, 141, 146), 901M14126 (135). All scale bars 5 µm, except 1 µm for 137 and 143.

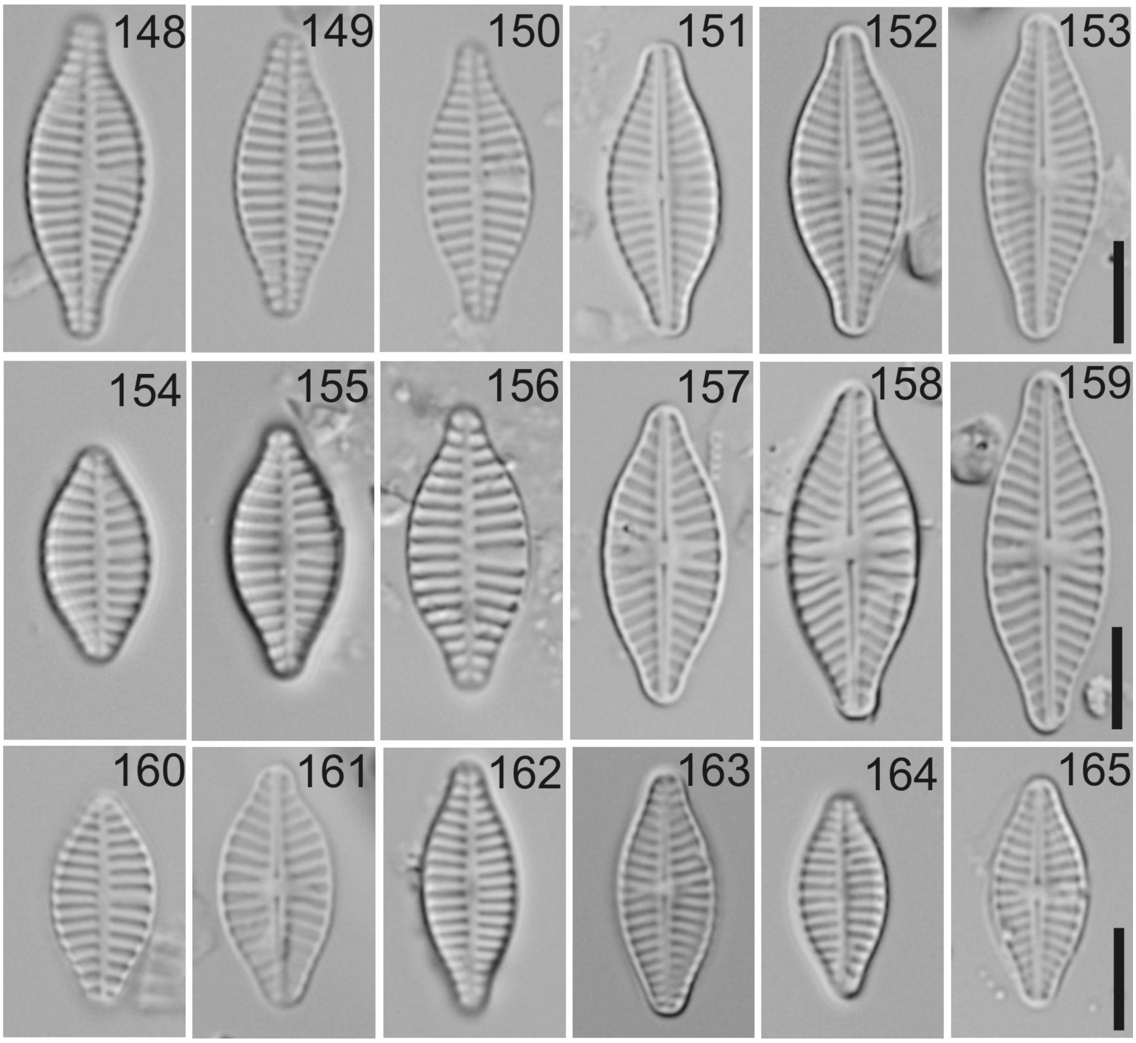

FIGURE 148–165. *P. delicatulum* (148–161) and *Planothidium* sp. 2 (162–165) LM. Samples: 901M14126 (148–153), 412M08599 (155–159), SMC03019 (154, 160, 161), 504PS0739 (162–165). All scale bars: 5 µm.

Planothidium delicatulum (Kützing) Round & Bukhtiyarova 1996

The valves are elliptical with protracted to cuneate-rostrate apices (Figs 148–161). The SV has a narrow, linear axial area, without a distinct central area (Figs 148–150, 154–156), but often unilaterally expanded due to the shortening of a central stria (Figs 148, 170) or a gap between the central striae (Figs 149, 150, 155, 156, 166). The RV has a narrow, linear axial area and small transversely rectangular central area, bordered by 2–3 slightly shortened striae on both sides (Figs 151–153, 157–159). Striae are parallel to weakly radiate on the SV and radiate on the RV.

SEM: The RV striae are more conical with 4 to 5, rarely 6 rows of same sized areolae, reduced to 1 or 2 near the tips (Figs 167–169). Striae separated by slightly raised virgae externally (Fig. 169). The SV has 4–5, rarely 6 rows of areolae (Figs 166, 170, 171).

Comments: This morphotype corresponds well with *P. delicatulum* valve morphology, ultrastructure and dimensions from the type material and from creek in France provided by Van de Vijver *et al.* (2018, Figs 1, 2, 72–98; valve size range: 5.5–8.5 µm wide, up to 20 µm long, 13–14 striae in 10 µm). However, there was a variation in the striae density and thickness in *P. delicatulum* populations from different streams in California, in some specimens, exceeding 14 striae in 10 µm.

Planothidium sp. 2

This morphotype (Figs 162–165) was separated from *P. delicatulum* based on slender valves, denser striae, and absent central gap on SV (Figs 162, 164).

Planothidium robustum (Hustedt) Lange-Bertalot 1999

The valves are elliptical with rostrate to distinctly capitate apices (Figs 172–186). The SV with narrow, linear to lanceolate axial area, without central area (Figs 172–176, 183, 185), but is often unilaterally expanded due to gap between the central striae (Figs 172–174, 176, 183). The RV has a linear axial area and a large elliptical central area, bordered by 4–7 distinctly shortened striae on both sides (Figs 177–181, 182, 184, 186). Striae are parallel to weakly radiate on SV and strongly radiate on RV.

SEM: The SV striae have parallel sides, composed of 4 to 6 rows of areolae (Figs 187–189). RV striae conical with 4 to 6 rows of same sized areolae, reduced to 1 or 2 near the tips (Figs 190–192). Striae separated by distinctly raised virgae externally, which often extend into central area. Transverse marks (depression lines) extending from the central striae are observed externally in some specimens (Fig. 192), visible with LM (Fig. 177).

Comments: This morphotype corresponds best to *P. robustum* (syn. *Achnanthes delicatula* var. *robusta* Hustedt 1934). Hustedt (1934) illustrated two valves of *A. delicatula* var. *robusta* (p. 378, Figs 1, 2 as follows: width 9 µm, length 24 µm, 13–14 striae in 10 µm). Lange-Bertalot & Krammer (1989) provided LM images of the holotype of *Achnanthes delicatula* var. *robusta* Hustedt (Tafel 80, Fig. 15, 15'). *P. australe* (Mangium) Le Cohu (syn. *Achnathes delicatula* var. *australis* Manguin 1954) as described by Le Cohu 2005 (p. 90, Figs 56–60, i.e. width 8–9 µm, length 6–29 µm, 13–14 striae in 10 µm) could be conspecific with *P. robustum*. However, only large specimens were assigned to both species by Hustedt (1934) and Le Cohu (2005), and therefore valve diminution may not be known. The smaller specimens from California have denser striae and smaller central area on RV, but their valve outline is typical for *P. robustum*. Many of the large valves have LM distinguishable transverse wrinkles in the central area (Fig. 179).

Planothidium species distribution

Distribution maps for each species are presented in Figure 193 and Supplemental Figure 6. Information on the number of samples, where species was recorded (n) is provided in Table 1. The most common and abundant *Planothidium* species, recorded across the entire state were *P. frequentissimum* (n=172, Fig. 193 B), *P. lanceolatum* (n=163, Fig. 193 A), *P. victorii* (Fig. 193 F) and *P. cryptolanceolatum* (Fig. 193 E, n=57 for each), *P. amphibium* (n=33, Fig. 193 I) and *P. minutissimum* (n=20, Fig. 193 D). Some species were concentrated in the coastal streams of Southern California, and only sporadically recorded in Northern California (i.e. *P. robustum*, n=61, Fig. 193 G, *P. engelbrechtii*, n=41, Fig. 193 K, *P. delicatulum*, n=15, Fig. 193 C), in contrast to *P. potapovae* (n=9, Fig. 193 H), observed only in Northern California. Two relatively common species, e.g. *P. amphibium* and *P. engelbrechtii,* were characteristic for non-perennial streams often exposed to desiccation, where they reached high abundance. Some rare taxa, such as *P. sheathii, P. incuriatum, P. tujii,* and *P. daui* have been recorded only in large rivers in Central and Northern California so far (Supplemental Figure 6).

Planothidum species environmental ranges and weighted averages

Species environmental ranges and weighted averages (WAs) for five environmental variables (chloride, conductivity, DOC, TN and TP) are presented in Figures 194 to 198. The paired randomization test comparisons of WAs for each species was done separately for each of the five environmental variables that were analyzed allowing for interspecies comparisons relative to each variable. We identified 57 significant interspecies differences across the data set. Matrices of p-values indicating which pair of species differ for each variable are presented in Supplemental Figures 1–5.

Species ranges overlapped along the chloride gradient which span from 0.09 to 3300 (median 39.6) mg/L (Fig. 194). *P. delicatulum, P. robustum, P. engelbrechtii, P. frequentissimum* and *P. victorii* showed largest ranges and highest WAs along the chloride gradient, opposed to *P. potapovae, Planothidium* sp. 1and *P. amphibium* with a narrower ranges and lowest WAs. *P. potapovae* maintained the greatest number of significant differences (6) with lowest WA (0.81 mg/L), while *P. delicatulum* showed the highest WA (256.26 mg/L).

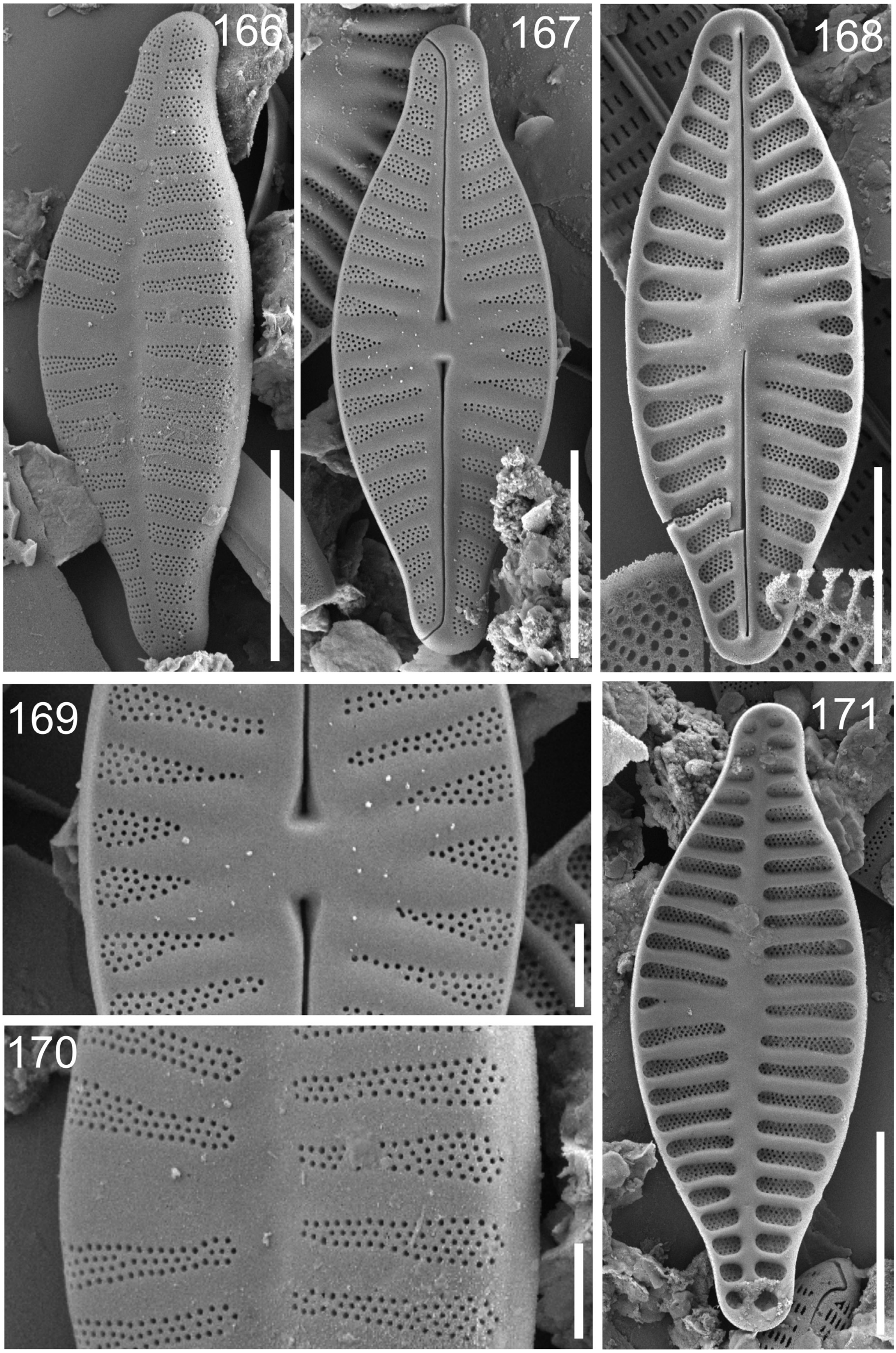

FIGURE 166–171. *P. delicatulum* SEM. Sample 901M14126. Scale bars: 5 µm (166–168, 171), 1 µm (169, 170).

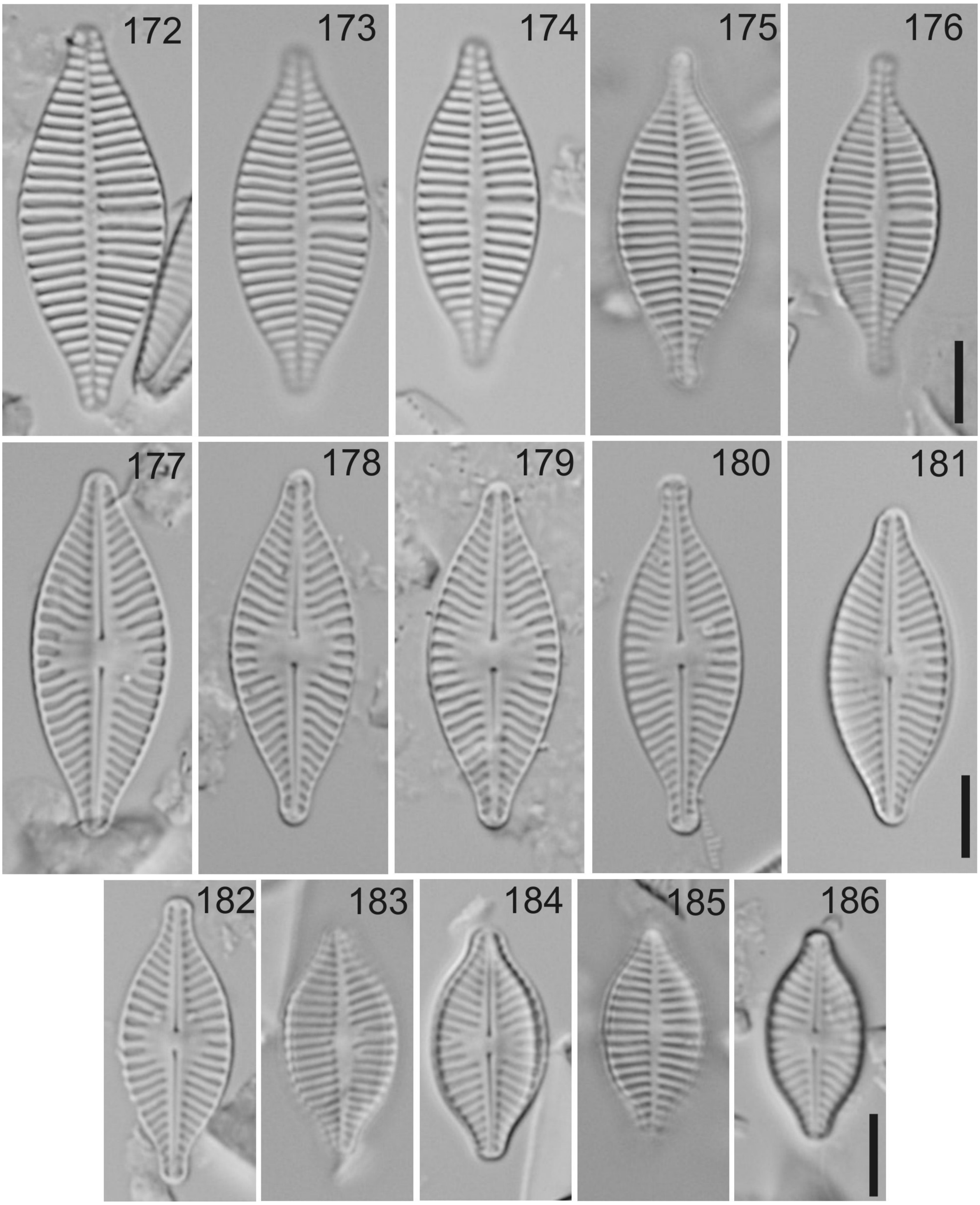

FIGURE 172–186. *P. robustum* LM. Samples: SMC00873 (172, 175, 178–180, 182)), 901M14126 (173, 174, 176, 177, 181), SMC03019 (183–186). All scale bars: 5 µm.

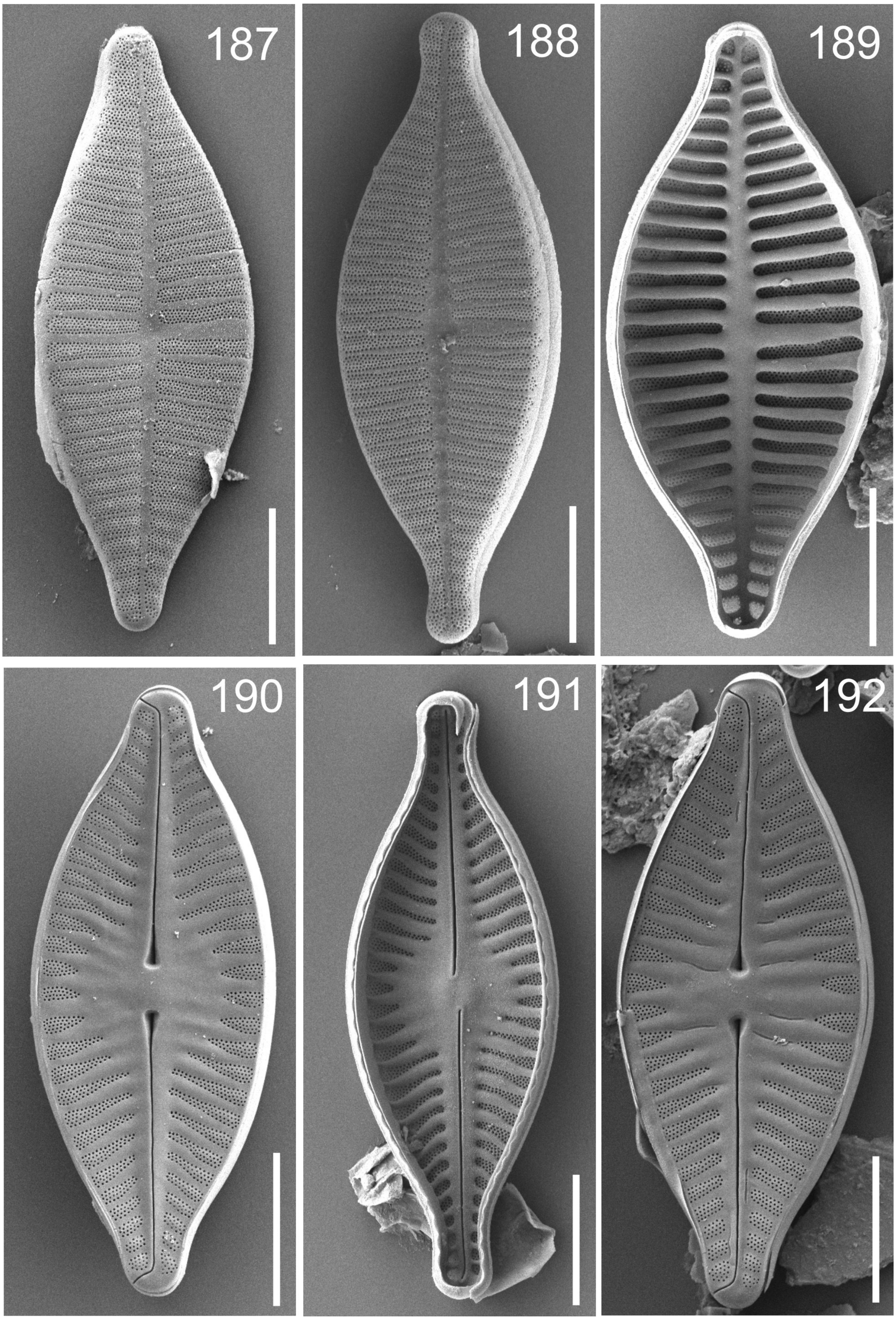

FIGURE 187–192. *P. robustum* SEM. Sample: SMC00873 (187, 188, 190–192), 901M14126 (189). All scale bars: 5 µm.

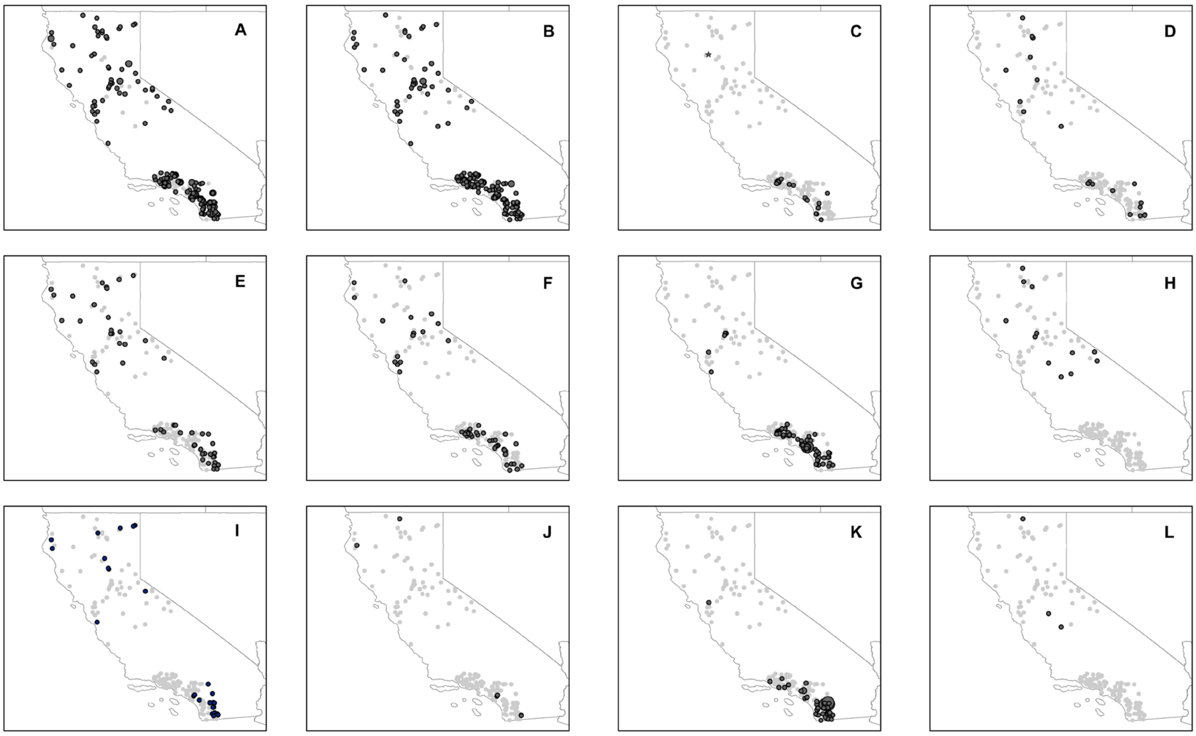

FIGURE 193. Distributional maps of the most common *Planothidium* species in streams and rivers in California. Black dots indicate sites where species was present, and grey dots indicate sites, where species was absent. Legend: (A) *P. lanceolatum*, (B) *P. frequentissimum*, (C) *P. delicatulum* and *Planothidium* sp. 2 (star), (D) *P. minutissimum*, (E) *P. cryptolanceolatum*, (F) *P. victorii*, (G) *P. robustum*, (H) *P. potapovae*, (I) *P. amphibium*, (J) *Planothidium* sp. 1, (K) *P. engelbrechtii*, (L) *P. rostratoholarcticum.*

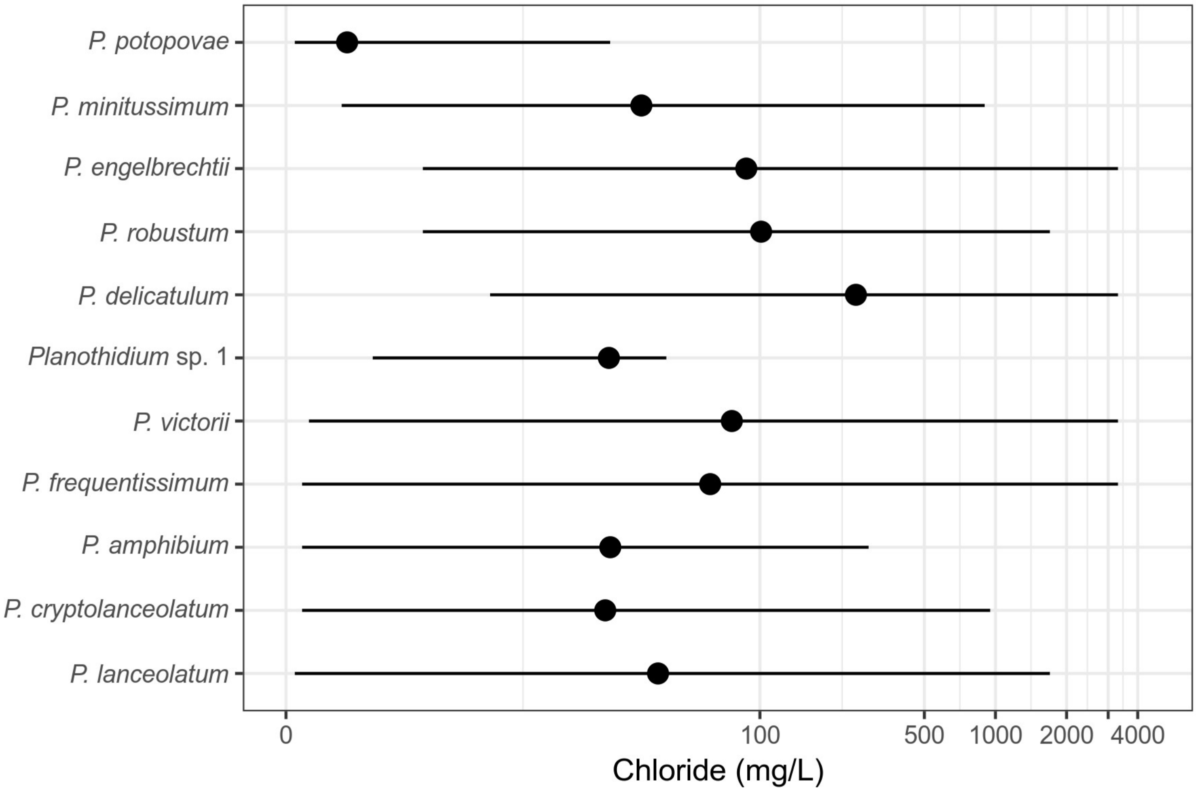

FIGURE 194. *Planothidium* species ranges (plotted as horizontal lines) and weighted averages (indicated by dot on each line) for chloride. Environmental variables are plotted on a log base 10 axis.

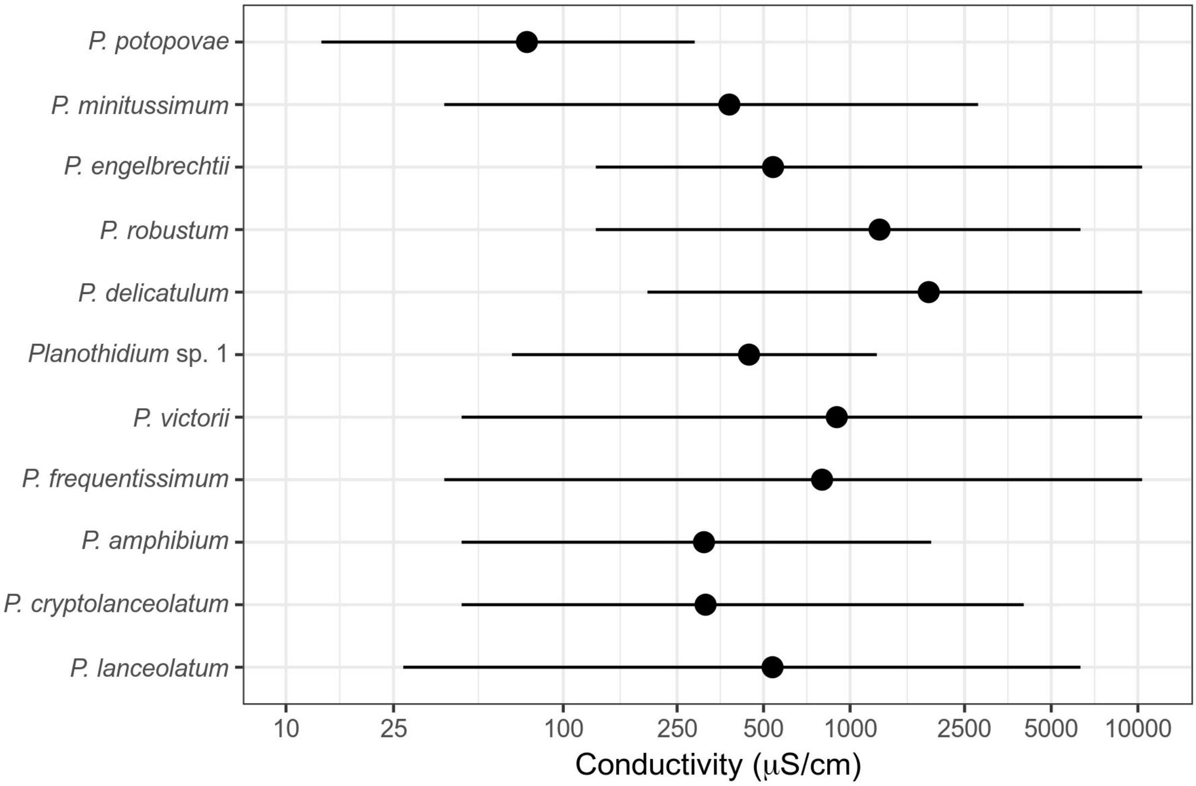

FIGURE 195. *Planothidium* species ranges (plotted as horizontal lines) and weighted averages (indicated by dot on each line) for conductivity. Environmental variables are plotted on a log base 10 axis.

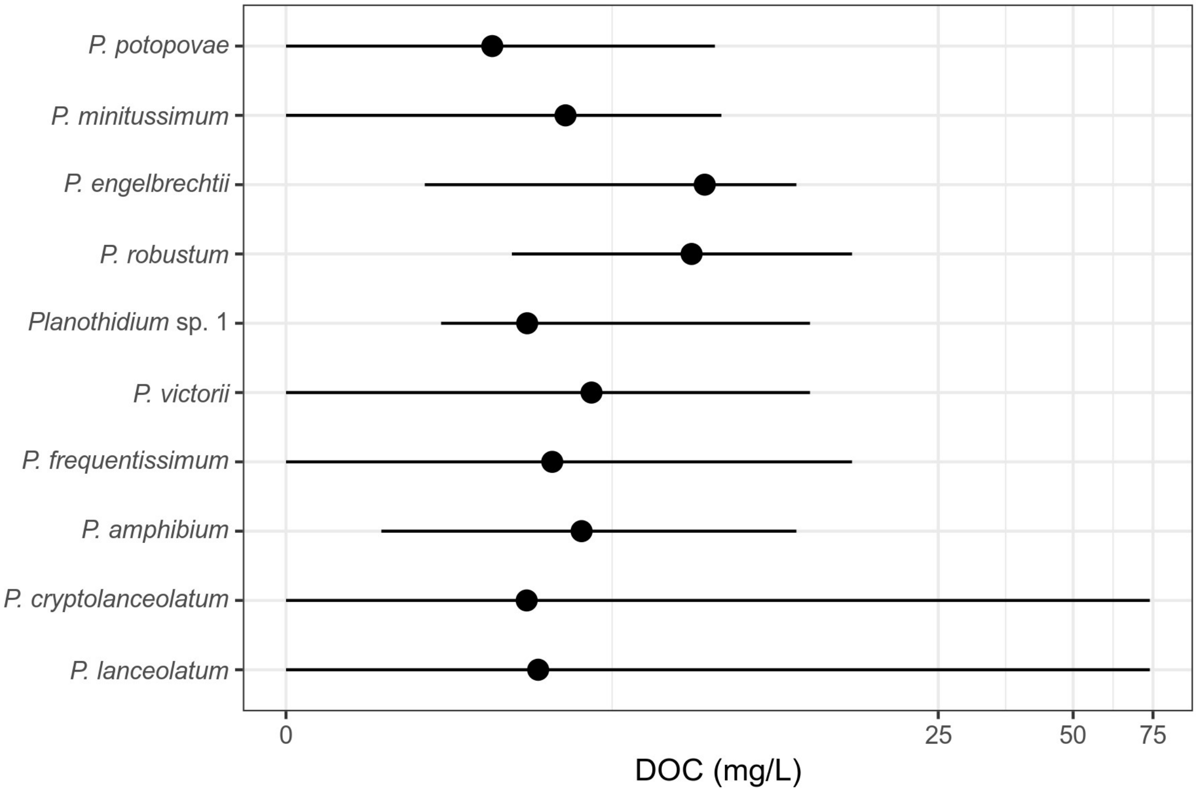

FIGURE 196. *Planothidium* species ranges (plotted as horizontal lines) and weighted averages (indicated by dot on each line) for DOC. Environmental variables are plotted on a log base 10 axis.

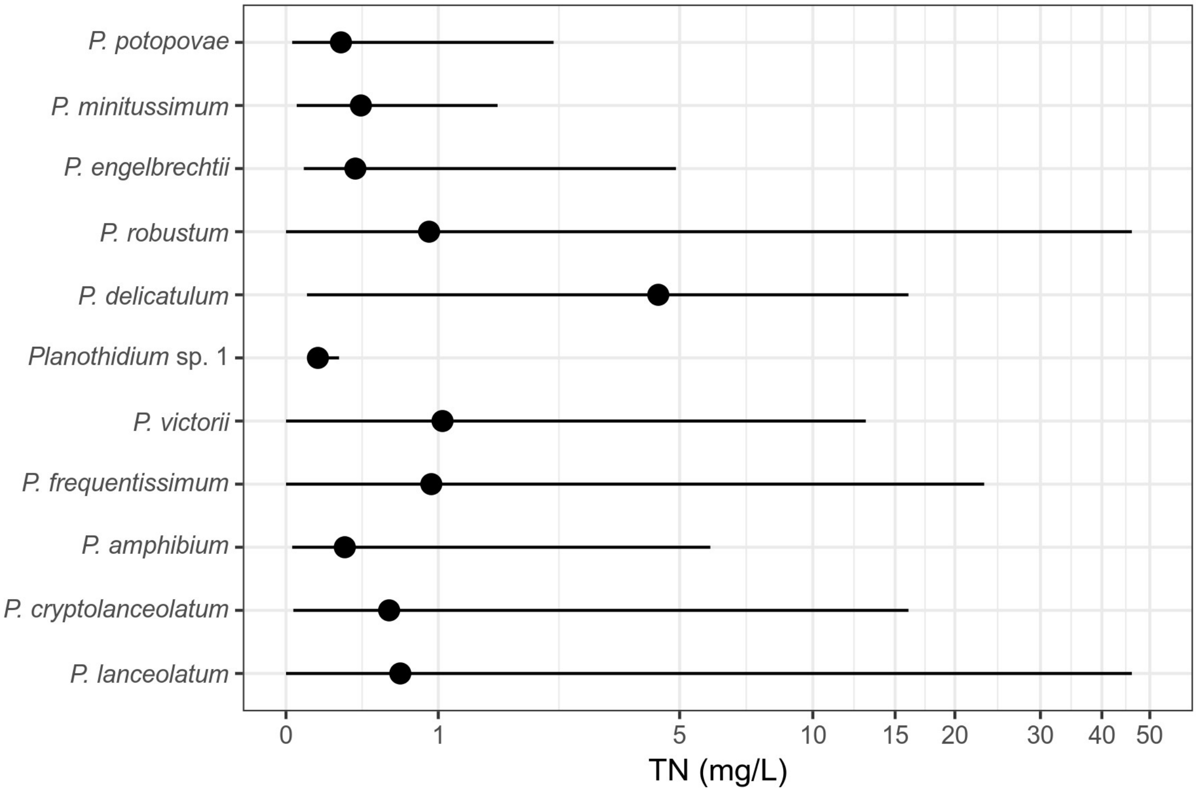

FIGURE 197. *Planothidium* species ranges (plotted as horizontal lines) and weighted averages (indicated by dot on each line) for TN. Environmental variables are plotted on a log base 10 axis.

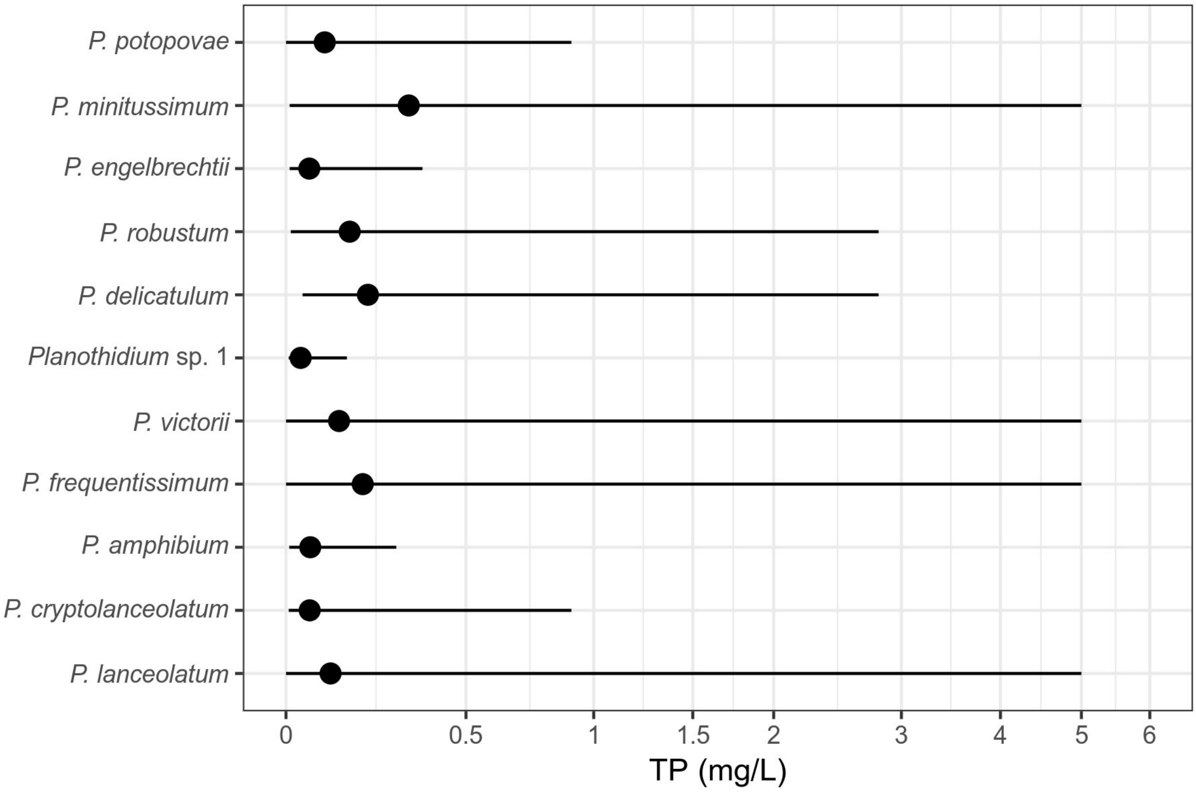

FIGURE 198. *Planothidium* species ranges (plotted as horizontal lines) and weighted averages (indicated by dot on each line) for TP. Environmental variables are plotted on a log base 10 axis.

Similarly, for conductivity (range 13.6 to 10344, median 805 µS/cm, Fig. 195), *P. delicatulum, P. robustum, P. engelbrechtii, P. frequentissimum* and *P. victorii* showed largest ranges and highest WAs, opposed to *P. potapovae, Planothidium* sp. 1 and *P. amphibium* with a narrower ranges and lowest WAs. *P. potapovae* showed the greatest number of significant differences from other species (7) and lowest WA (74.5 µS/cm), while *P. delicatulum* showed the highest WA (1876.6 µS/cm).

In the case of DOC (range 0 to 73.8, median 2.67 mg/L, Fig. 196), *P. engelbrechtii* showed the most significant differences (6) from other species with highest WA (7.1 mg/L), in contrast to *P. potapovae* with lowest WA (1.8 mg/L).

With respect to TN (range 0 to 46, median 0.352 mg/L, Fig. 197), the species with lowest WA was *Planothidium* sp. 1 (0.16 mg/L), and with highest was *P. delicatulum* (4.44 mg/L). *P. frequentissimum* (WA 0.94 mg/L) showed the most significant differences from six species with lowest WA, e.g. *P. amphibium, P. cryptolanceolatum, P. engelbrechtii, Planothidium s*p. 1. *P. minutissimum,* and *P. potapovae*.

Similarly, *P. frequentissimum* (WA for TP 0.19 mg/L) showed the most significant differences along the TP gradient (range 0 to 5, median 0.065 mg/L, Fig. 198), from seven species with lowest WAs, e.g. *P. amphibium, P. cryptolanceolatum, P. lanceolatum, P. engelbrechtii, Planothidium* sp. 1*, P. potapovae* and *P. victorii*. The species with lowest WA was *Planothidium* sp. 1(0.03 mg/L), and the species with the highest WA was *P. minutissimum* (0.32 mg/L). The species with narrower ranges towards the low end of both TN and TP gradients were *P. potapovae, Planothidium* sp. 1*, P. amphibium,* and *P. engelbrechtii.*

Discussion

For this study we applied the most recent *Planothidium* taxonomy (Jahn *et al.* 2017, Van de Vijver *et al.* 2018, Wetzel *et al.* 2013, 2019), which is providing a new classification system of the extensive morphological variation within the genus. As result, we identified 20 infrageneric *Planothidium* taxa from streams and rivers in California, including one new to science species, i.e. *Planothidium californicum*. Most of the identifications have been supported with SEM data, which showed the diagnostic importance of some ultrastructure features is pecies identification (e.g., areolae number and pattern in the striae). For instance, two recently described species—*P. sheathii* (Stancheva 2019) and *P. hintzianum* (Wetzel *et al.* 2019) have very similar frustule gross morphology, but the striae in *P. sheathii* appear thicker under LM, because contain much more rows of areolae. Furthermore, SEM revealed the consistent presence of minor details with unknown taxonomic value, such as external disordered marks (depression lines) on SV in some species (see *P. potapovae* on Fig. 82 and *P. hinzianum* on Fig. 85), reported previously by Wetzel *et al.* 2019 (Figs 239, 240, 243, 457, 458). Similar marks (depression lines), but transverse are observed on RV of *P. robustum* (Fig. 192). Detailed LM documentation of the *Planothidium* flora provided here will facilitate further identifications and taxonomic consistency within SWAMP bioassessment program in California and could serve as potential link between morphological and future molecular species identifications, when anticipated sequence data from the studied dataset become available.

Refined knowledge about the local environmental preferences of diatom taxa is crucial for bioassessment studies, because they are the foundation of diatom indices for evaluation of the stream health in California (Fetscher *et al.* 2014). However, the local diatom indices currently include *P. lanceolatum* and *P. frequentissimum* as species complexes, associated with high TP and TN indicator values determined from other eco-regions in the USA (e.g., Potapova & Charles 2007). This study, which applied more refined taxonomy, showed differences in ecological preferences of the members of both species complexes. For instance, *P. cryptolanceolatum* had slightly narrower environmental ranges and lower WAs than *P. lanceolatum* for all five gradients, although not significantly. Furthermore, *P. lanceolatum* was the most indifferent *Planothidium* species, with only a single significant difference (from *P. frequentissimum*, regarding TP), while *P. cryptolanceolatum* was more sensitive, with significantly lower WAs for chloride and conductivity from *P. frequentissimum, P. victorii* and *P. robustum*, for DOC from *P. engelbrechtii*, and for TN and TP from *P. frequentissimum*. Similarly, separating two species from the *P. frequentissimum* species complex (i.e. *P. victorii* and *Planothidium* sp. 1) revealed their contrasting preferences for TN and organic load. Furthermore, both species had significantly lower TN and TP WAs compared to *P. frequentissimum.*

Another pair of morphologically similar species, which often occurred together in coastal streams in Southern California were *P. delicatulum* and *P. robustum*. Both species were previously classified as indicators of high TN and TP for inland waters in the USA (Potapova & Charles 2007). *P. delicatulum* is also known as widespread in brackish and marine habitats (Van de Vijver *et al.* 2018). However, this study indicated that *P. robustum* is more sensitive than *P. delicatulum* to anthropogenic pressure locally, considering it is consistently lower WAs (although not significantly) for chlorides, TN and TP.

This study also provided a signal for different desiccation tolerances among *Planothidium* species, with *P. amphibium* and *P. engelbrechtii* characteristic and particularly abundant in non-perennial streams in Southern California, able to colonize variable substrates, including large colonial diatoms as *Eunotia pectinalis* (Kützing) Rabenhorst and *Pleurosira laevis* (Ehrenberg) Compère. Our observation is in agreement with Wetzel *et al.* (2014) who recorded *P. amphibium* to be most abundant in moist terrestrial habitats in the sampling area in Oregon, USA. Interestingly, *P. amphibium* and *P. engelbrechtii* showed preferences for low nutrients, but high dissolved organic compounds in the water. The source of organic compounds in these intermittent streams, which are typically high-quality low-order streams in remote areas, could be the green, red and golden benthic macroalgae, which produce abundant extracellular mucilage (Stancheva and Lowe 2019c).

In contrast, some rare taxa were rarely recorded only in large rivers, such as *P. sheathii* (Stancheva 2019), *P. incuriatum* and *P. tujii*. Geographical trends in *Planothidium* distribution were observed as well, with species predominantly recorded in Southern California (e.g. *P. delicatulum*, *P. robustum, P. engelbrechtii*), or Northern California (e.g., *P. potapovae*).

In conclusion, this work demonstrated the benefits of detailed taxonomic separation of diatom species complexes and their consistent identifications across large data sets in order to improve the knowledge about species ecological preferences and to enhance the power of diatom-based bioassessment.

Acknowledgements

The California State Water Resources Control Board Surface Water Ambient Monitoring Program and the Stormwater Monitoring Coalition who provided samples and funding for this study. The authors acknowledge the assistance in scanning electron microscopy by Paul Warren at the Nano3 Facility at the University of California, San Diego. The authors are thankful to Prof. Regine Jahn, Botanischer Garten und Botanisches Museum Berlin-Dahlem, Berlin, Germany for providing opinion on *Planothidium californicum* taxonomic identity as a new species and to Bart Van de Vijver, Meise Botanic Garden, Meise, Belgium for discussion on *Planothidium engelbrechtii* species complex. We thank the editor Dr. Evan Thomas and anonymous reviewer for their valuable comments, which improved the presentation of this paper.

References

Álvarez-Blanco, I. & Blanco, S. (2013) *Planothidium galaicum sp. nov.* (Bacillariophyta, Achnanthidiaceae), a new diatom species from Galician coast, Spain. *Phytotaxa* 151: 44–52.
https://doi.org/10.11646/phytotaxa.151.1.4

Bąk, M. & Lange-Bertalot, H. (2014) Four small-celled *Planothidium* species from Central Europe proposed as new to science. *Oceanological and Hydrobiological Studies* 43: 346–359.
https://doi.org/10.2478/s13545-014-0152-9

Blanco, S., Álvarez-Blanco, I., Cejudo-Figueiras, C., Recio Espejo, J.M., Borja Barrera, C., Bécares, E., Díaz del Olmo, F. & R.Cámara Artigas (2013) The diatom flora in temporary ponds of Doñana National Park (southwest Spain): five new taxa. *Nordic Journal of Botany* 31: 489–499.
https://doi.org/10.1111/j.1756-1051.2013.01691.x

Cantonati, M., Kelly, M.G. & Lange-Bertalot, H. (2017) *Freshwater benthic diatoms of Central Europe: over 800 common species used in ecological assessments. English edition with updated taxonomy and added species.* Koeltz Botanical Books, Schmitten-Oberreifenberg, 1–942 pp. 135 pls.

Carter, J.R. (1966) Some freshwater diatoms of Tristan da Cunha and Gough Island. *Nova Hedwigia* 11: 443–483.

Cholnoky, B.J. (1955) Diatomeen aus salzhaltigen Binnengewässern der westlichen Kaap-Provinz in Südafrika. *Berichte der Deutschen Botanischen Gesellschaft* 68: 11–23.

Compère, P. & Van de Vijer, B. (2009) *Planothidium engelbrechtii* (Cholnoky) Round & Bukhtiyarova: Identity and lectotypification (Bacillariophyta). *Fottea* 9: 187–192.
https://doi.org/10.5507/fot.2009.019

Fetscher, A.E., Busse, L. & Ode, P.R. (2009) *Standard Operating Procedures for Collecting Stream Algae Samples and Associated Physical Habitat and Chemical Data for Ambient Bioassessments in California.* California State Water Resources Control Board Surface Water Ambient Monitoring Program (SWAMP) Bioassessment SOP 002. (updated May 2010). Available from: http://www.waterboards.ca.gov/water_issues/programs/swamp/docs/sop_algae.pdf (accessed 2 November 2020)

Fetscher, A.E., Stancheva, R., Kociolek, J. P, Sheath, R.G., Stein, E.D., Mazor, R.D., Ode, P.R. & Busse, L.B. (2014) Development and comparison of stream indices of biotic integrity using diatoms *vs.* non-diatom algae *vs.* a combination. *Journal of Applied Phycology* 26: 433–450.
https://doi.org/10.1007/s10811-013-0088-2

Hering, D., Borja, A., Jones, J.I., Pont, D., Boets, P., Bouchez, A., Bruce, K., Drakare, S., Hänfling, B., Kahlert, M., Leese, F., Meissner, K., Mergen, P., Reyjol, Y., Segurado, P., Vogler, A. & Kelly, M. (2018) Implementation options for DNA-based identification into ecological status assessment under the European Water Framework Directive. *Water Research* 138: 192–205.
https://doi.org/10.1016/j.watres.2018.03.003

Hustedt, F. (1934) Die Diatomeenflora von Poggenpohls Moor bei Dötlingen in Oldenburg. *Abhandlungen und Vorträgen der Bremer Wissenschaftlichen Gessellschaft* 8/9: 362–403.

Jahn, R., Abarca, N., Gemeinholzer, B., Mora, D., Skibbe, O., Kulikovskiy, M., Gusev, E., Kusber, W.H. & Zimmermann, J. (2017) *Planothidium lanceolatum* and *Planothidium frequentissimum* reinvestigated with molecular methods and morphology: four new species and the taxonomic importance of the sinus and cavum. *Diatom Research* 32: 75–107.
https://doi.org/10.1080/0269249X.2017.1312548

Krammer, K. & Lange-Bertalot, H. (1991) Bacillariophyceae. 4 Teil. Achnanthaceae. Kritische Ergänzungen zu *Navicula* (Lineolatae) und *Gomphonema*.- Die Süsswasserflora von Mitteleuropa 2/4. Jena: Gustav Fischer Verlag. 437 pp.

Lange-Bertalot, H. & Krammer, K. (1989) *Achnanthes*, eine Monographie der Gattung mit Definition der Gattung *Cocconeis* und Nachtragen zu den *Naviculaceae*. *Bibliotheca Diatomologica* 18: 1–393.

Le Cohu, R. (2005) Révision des principales espèces dulçaquicoles d'Achnanthales (Bacillariophyta) des îles subantarctiques de Kerguelen [Revision of the main freshwater species of *Achnanthales* (Bacillariophyta) from sub–antarctic Iles Kerguelen]. *Algological Studies* 116: 79–114.
https://doi.org/10.1127/1864-1318/2005/0116-0079

Lowe, R.L. & Cody, W.R. (2002) *Planothidium rostratum* (Østrup) Lange-Bertalot (Bacillariophyceae) and related species from North American streams and rivers. *In:* Morales, E.A. & Charles, D.F. (Eds.) *Tenth NAWQA Taxonomy Workshop on Harmonization of Algal Taxonomy June 13–15, 200263-87. Report No. 05-1F.* Phycology Section/Diatom Analysis Laboratory, Patrick Center for Environmental Research, The Academy of Natural Sciences of Philadelphia, Philadelphia, pp. 63–87.

Mora, D., Carmona, J., Jahn, R., Zimmermann, J. & Abarca, N. (2017) Epilithic diatom communities of selected streams from the Lerma-Chapala Basin, Central Mexico, with the description of two new species. *Phytokeys* 88: 39–69.
https://doi.org/10.3897/phytokeys.88.14612

Morales, E.A. (2006) Small *Planothidium* Round et Bukhtiyarova (Bacillariophyceae) taxa related to *P. daui* (Foged) Lange-Bertalot from the United States. *Diatom Research* 21: 325–342.
https://doi.org/10.1080/0269249X.2006.9705673

Moss, M.O. & Carter, J.R. (1982) The resurrection of *Achnanthes rostrata* Ostrup. *Bacillaria* 5: 157–164.

Novis, P., Braidwood, J. & Killroy, C. (2012) Small diatoms (Bacillariophyta) in cultures from the Styx River, New Zealand, including descriptions of three new species. *Phytotaxa* 64: 11–45.
https://doi.org/10.11646/phytotaxa.64.1.3

Potapova, M. & Charles, D.F. (2007) Diatom metrics for monitoring eutrophication in rivers of the United States. *Ecological Indicators* 7: 48–70.
https://doi.org/10.1016/j.ecolind.2005.10.001

Potapova, M. (2011a) *Planothidium dubium*. *In: Diatoms of North America.* Available from: https://diatoms.org/species/planothidium_dubium (accessed 20 June 2018)

Potapova, M. (2011b) *Planothidium hainaldii*. *In: Diatoms of North America.* Available from: https://diatoms.org/species/planothidium_hainaldii (accessed 20 June 20 2018)

Rehn, A.C. (2016) Using Multiple Biological and Habitat Condition Indices for Bioassessment of California Streams (Technical memo No. SWAMP-TM-SB-2016-0003). State Water Resources Control Board Surface Water Ambient Monitoring Program, Sacramento, CA. [https://www.waterboards.ca.gov/water_issues/programs/swamp/bioassessment/docs/multiple_indices_tech_memo.pdf]

Round, F.E. & Bukhtiyrova, L. (1996a) Epipsammic diatoms – communities of British rivers. *Diatom Research* 11: 363–372.

https://doi.org/10.1080/0269249X.1996.9705390

Round, F.E. & Bukhtiyarova, L. (1996b) Four new genera based on *Achnanthes (Achnanthidium)* together with a re-definition of *Achnanthidium*. *Diatom Research* 11: 345–361.
https://doi.org/10.1080/0269249X.1996.9705389

Rumrich, U., Lange-Bertalot, H. & Rumrich, M. (2000) Diatomeen der Anden. Von Venezuela bis Patagonien (Feuerland). *Iconographia Diatomologica* 9: 1–649.

Spaulding, S.A., Edlund, M.B. & Metzeltin, D. 2008. *Planothidium*. *In: Diatoms of the United States*. Available From: https://diatoms.org/genera/planothidium/guide.

Smucker, N.J., Detenbeck, N.E. & Morrison, A.C. (2013) Diatom responses to watershed development and potential moderating effects of near-stream forest and wetland cover. *Freshwater Science* 32: 230–249.
https://doi.org/10.1899/11-171.1

Stancheva, R., Busse, L., Kociolek, J.P. & Sheath, R.G. (2015) *Standard Operating Procedures for Laboratory Processing and Identification of Stream Algae*. California State Water Resources Control Board Surface Water Ambient Monitoring Program (SWAMP) Bioassessment SOP 0003. [http://www.waterboards.ca.gov/water_issues/programs/swamp/bioassessment/docs/sop_algae_lab.pdf]

Stancheva, R., Sheath, R.G. & Kociolek, J.P. (2016) New freshwater gomphonemoid diatoms from streams in the Sierra Nevada mountains, California, USA. *Phytotaxa* 289: 118–134.
https://doi.org/10.11646/phytotaxa.289.2.2

Stancheva, R. (2019a) *Cocconeis cascadensis*, a new monoraphid diatom from mountain streams in northern California, USA. *Diatom Research* 33: 471–484.
https://doi.org/10.1080/0269249X.2019.1571531

Stancheva, R. (2019b) *Planothidium sheathii*, a new monoraphid diatom species from rivers in California, USA. *Phytotaxa* 393: 131–140.
https://doi.org/10.11646/phytotaxa.393.2.4

Stancheva, R. & Lowe, R. (2019c). Diatom symbioses with other photoautotrophs. *In: Diatoms: Fundamentals and Applications*. Gordon, R. & Seckbach, J. (Eds.) Wiley-Scrivener Publishing, pp. 225–244.
https://doi.org/10.1002/9781119370741.ch10

USEPA (2017) National Rivers and Streams Assessment 2018/19: Field Operations Manual – NonWadeable. EPA-841-B-17-003b. U.S. Environmental Protection Agency, Office of Water Washington, DC.

Van de Vijver, B., Wetzel, C.E., Kopalová, K., Zidarova, R. & Ector, L. (2013) Analysis of the type material of *Achnanthidium lanceolatum* Brébisson ex Kützing (Bacillariophyta) with the description of two new *Planothidium* species from the Antarctic Region. *Fottea* 13: 105–117.
https://doi.org/10.5507/fot.2013.010

Van de Vijver, B., Wetzel, C.E. & Ector, L. (2018) Analysis of the type material of *Planothidium delicatulum* (Bacillariophyta) with the description of two new *Planothidium* species from the sub-Antarctic Region. *Fottea* 18: 200–211.
https://doi.org/10.5507/fot.2018.006

Van de Vijver, B., Wetzel, C.E. & Ector, L. (2019) *Planothidium pericavum/engelbrehtii* complex. Abstracts of the North American Diatom Meeting, University of Georgia Rock Eagle 4S, USA, pp. 56.

Werum, M. & Lange-Bertalot, H. (2004) Diatoms in springs from Central Europe and elsewhere under the influence of hydrologeology and anthropogenic impacts. *Iconographia Diatomologica* 13: 3–417, pls 1–105

Wetzel, C.E., Van de Vijver, B., Hoffmann, L. & Ector, L. (2013) *Planothidium incuriatum sp. nov.* a widely distributed diatom species (Bacillariophyta) and type analysis of *Planothidium biporomum*. *Phytotaxa* 138: 43–57.
https://doi.org/10.11646/phytotaxa.138.1.6

Wetzel, C.E., Van de Vijver, B., Kopalová, K., Hoffmann, L., Pfister, L. & Ector, L. (2014) Type analysis of the South American diatom *Achnanthes haynaldii* (Bacillariophyta) and description of *Planothidium amphibium sp. nov.*, from aerial and aquatic environments in Oregon (USA). *Plant Ecology and Evolution* 147: 439–454.
https://doi.org/10.5091/plecevo.2014.1058

Wetzel, C.E., Van de Vijver, B., Blanco, S. & Ector, L. (2019) On some common and new cavum bearing *Planothidium* (Bacillariophyta) species from freshwater. *Fottea* 19: 50–89.
https://doi.org/10.5507/fot.2018.016

Zimmermann, J., Abarca, N., Enke, N., Skibbe, O., Kusber, W.H. & Jahn, R. (2014) Taxonomic reference libraries for environmental barcoding: a best practice example from diatom research. *PLoS ONE* 9: e108793.
https://doi.org/10.1371/journal.pone.0108793